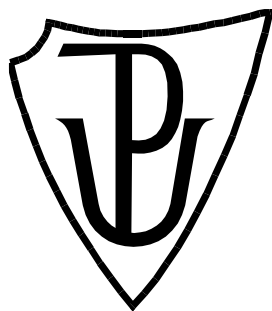# UNIVERZITA PALACKÉHO V OLOMOUCI

Přírodovědecká fakulta

Katedra biochemie

Effect of CuEt on murine T cells and its role in tumour cytotoxicity

DIPLOMOVÁ PRÁCE

Autor:	**Viktor Valentini**
Studijní program:	N0512A130009 - Biochemie
Studijní obor:	Biochemie
Forma studia:	Prezenční
Vedoucí práce:	**Juan Bautista De Sanctis Ph.D.**
Rok: :	2023

Prohlašuji, že jsem diplomovou práci vypracoval samostatně s vyznačením všech použitých pramenů a spoluautorství. Souhlasím se zveřejněním diplomové práce podle zákona č. 111/1998 Sb., o vysokých školách, ve znění pozdějších předpisů. Byl/a jsem seznámen/a s tím, že se na moji práci vztahují práva a povinnosti vyplývající ze zákona č. 121/2000 Sb., autorský zákon, ve znění pozdějších předpisů.

V Olomouci dne 28.7.2023
Viktor Valentini

Bibliografická identifikace

Jméno a příjmení autora	Bc. Viktor Valentini
Název práce	Efekt CuEt na myší T lymfocyty a jeho role v protinádorové cytotoxicitě
Typ práce	Diplomová
Pracoviště	IMTM-Institute of Molecular and Translational Medicine
Vedoucí práce	prof. Juan Bautista De Sanctis Ph.D.
Rok obhajoby práce	2023

Abstrakt:

Tato práce je zaměřená na aktivační účinek který mají nanomolární koncentrace CuEt na myší splénické T-lymfocyty a aktivaci signálních drah. V úvodní a teoretické části byla provedena rozsáhlá literární rešerše s cílem získání a předložení informací ohledně možných signalizačních drah a interakcí in dukovaných uvnitř buňky po ošetření CuEt. K experimentům byly použity myší kmeny BALB/c a C57BL6.

V experimentální části byly od sebe oděleny CD8+ a CD4+ buňky které byly pak ošetřeny zvlášť. Byla změřena fosforylace ERK1/2 a také exprese NKG2D(CD314) a perforinu. Po stimulaci je dráha ERK1/2 jasně fosforylována u CD8+ T-lymfocytů. U CD4+ ošetřených buněk byl tento efekt menší než v CD8+ buňkách. Bylo také potvrzeno, že nanomolární koncentrace CuEt zvyšuje expresi perforinu a NKG2D(CD314).

Počet stran	43
Jazyk	Anglický

Bibliographical identification

Autor's first name and surname	Bc. Viktor Valentini
Title	Effect of CuEt on murine T cells and its role in tumour cytotoxicity
Type of thesis	Diplomová
Department	IMTM-Institute of Molecular and Translational Medicine
Supervisor	prof. Juan Bautista De Sanctis Ph.D.
The year of presentation	2023

Abstract:

This thesis focuses on the priming effect nanomolar concentrations of CuEt have on murine splenic T-cells and the activation of signal pathways. In the introduction and theoretical part, extensive literary research was performed to gather and present information about the possible signalling pathways and interactions induced by the treatment with CuEt. The mice strains used for the experiments were BALB/c and C57BL6.

In the experimental part, CD8+ and CD4+ murine splenocytes were separated and treated separately. The phosphorylation of ERK1/2 and the expression of NKG2D(CD314) and perforin were measured. Upon stimulation, the ERK1/2 pathway is phosphorylated in CD8+ T-cells. In CD4+ treated cells, the effect was lower than in CD8+ cells. It was also confirmed that nanomolar concentrations of CuEt enhance perforin and NKG2D(CD314) expression.

Keywords	disulfiram metabolites, cytotoxicity, T cell cytotoxicity, NF-κB, CuEt, ERK1/2, STAT3, JAK, perforin, NKG2D, T-cell priming, CD8+, CD4+
Number of pages	43
Language	English

Aknowledgment

First, I would like to thank my thesis supervisor, prof. Juan Bautista De Sanctis, PhD, to whom I am very grateful for his never-ending patience and readiness to answer my many questions at any time. He was of incredible help, even in the worst of times, a person who taught me and showed me a lot. I would also like to thank Bc. Alex Puskásů was of great help in the SDS-PAGE and Western-blot part of the experiments.

Last but not least, I would like to thank my whole family for standing by me and being very supportive of everything I did. For helping me go through tough times and motivating me. Another thanks goes to Rebechin Caffè in the town Grado, whose hospitality allowed me to write this thesis in a friendly environment when I needed it the most.

TABLE OF CONTENTS

List of figures

List of graphs

List of abbreviations

ALDH	Aldehyde dehydrogenase
APC	Adenomatous polyposis coli
AP1	Activator protein 1
BSA	Bovine serum albumin
CuEt	Diethyldithiocarbamate copper
DEAB	D-aminobenzaldehyde
DNA	Deoxyribonucleic Acid
DSF	Disulfiram
ERK	Extracellular signal-regulated kinase
FBS	Fetal bovine serum
HIES	Hyper IgE syndrome
HLA	Human leukocyte antigen
HRP	Horseradish peroxidase
IFNγ	Interferon gamma
IL	Interleukin
IKK	IκB kinase complex
IRF	Interferon regulatory factor
JNK	c-Jun N-terminal kinase
KIR	Kill inhibitory receptor
LCK	Leukocyte specific kinase
LDL	Low density lipids
LIR	Leukocyte Ig-like receptors
MAPK	Mitogen activated protein kinase
MDSC	Myeloid-derived suppressor cells
Me-DTC-SO	S-methyl-N, N-diethyldithiocarbamate-sulfoxide
MHC-I/II	Major histocompatibility complex class 1/2
MICA/B	MHC class I chain-related proteins A and B
NF-κB	Nuclear factor kappa B
NK	Natural killer cell
NKG2D	Natural killer group 2 member D receptor
NKT	Natural killer T cell

PD-1	Programmed cell death protein 1
ROS	Reactive oxygen species
RPM	Revoltions per minute
STAT	Signal transducer activator of transcription
TCR	T-cell receptor
TNF	Tumor necrosis factor
UV	Ultraviolet light

1 Introduction

Major histocompatibility complex class I (MHC-I) molecules are transmembrane glycoproteins presenting peptides inside the cell. MHC-I presents endogenous peptides which can be recognised by CD8+ and NK cells. Self-antigens are differentiated from non-sef antigens; the cell is spared when an immune cell binds to it and recognises the peptide as its own. On the contrary, when the peptide is deemed foreign, the immune cell initiates a process to eliminate the cell (A. Halenius *et al.,* 2015).

NK cells express killer cell immunoglobulin-like receptors (KIRs) and leukocyte Ig-like receptors (LIRs). Both bind to MHC I molecules and mainly inhibit NK cell activation depending on the intracellular signal array. If the MHC I molecules expressed in the cells are low, then the cell's destruction is more likely (A. Halenius *et al.,* 2015). CD1 is another important molecule similar to MHC-I that activates T cell subpopulations (M. A. Exley *et al.,* 2021).

Moreover, there are non-classical MHC molecules (HLA-E/F/G, MICA/B etc.) that aren't as conserved and are usually recognised by different receptors such NKG2A, NKG2C NKG2D (A. Halenius *et al.,* 2015; G. Kochan *et al.,* 2013). The immune system can prevent the creation and proliferation of cancer cells by selectively targeting them based on their MHC expressed. One such mechanism relies on the non-classical MHC class I chain-related proteins A and B (MICA/B). These proteins, along with six glycoproteins from the ULBP family (ULBP1-6), are ligands for the natural killer group 2 member D (NKG2D) receptor (Y. Kim *et al.* 2020). MICA ligands aren't generally expressed in healthy human cells; they are expressed only when a cell is stressed or damaged, such as heat shock, viral infection, or cancer transformation. MICA are similar to heat-shock proteins and can become soluble (S. Holdenrieder *et al.,* 2006; K. Prajapati *et al.* 2018). NKG2D is a receptor mainly expressed by NK and CD8+ T-cells and a small subpopulation of CD4+ T-cells (K. Prajapati *et al.* 2018). When NKG2D binds to a ligand such as MICA, NK cells initiate a kill response.

Interestingly in CD8+ T-cells, NKG2D is a co-stimulatory signal that enhances T-cell function and activation. Simultaneous T-cell receptor (TCR) activation is needed for maximum cell activation (K. Prajapati *et al.* 2018). A study by Hu *et al.* in 2016 confirmed that CD28 activation on CD8+ T-cells leads to sustained activation of the tyrosine kinase Lck which in turn activates the Janus kinase (JAK), leading to STAT3 phosphorylation and ultimately to the upregulation of expression of NKG2D on CD8+ T-cells. The role of STAT3 in NKG2D

expression was also confirmed in human and murine NK cells by Zhu *et al.* in 2014. This study showed IL-10 and IL-21 enhanced STAT3 phosphorylation, leading to higher NKG2D expression. In this study, we aim to investigate whether the priming effect of CuEt on CD8+ and CD4+ T-cells, respectively, is due to a similar upregulation of NKG2D like the one that occurs with CD28 stimulation through STAT3 signalling and a higher expression and production of perforin due to NF-κB and ERK1/2 signalisation or another theory is the possible change of immune cell population differentiation and regulation through cytokine and STAT signalling leading to a possible lower amount or activity of T-reg cells. If this were the case, then it would make immune evasion of tumours in their microenvironments much harder. These mechanisms might be viable, and CuEt might have a dual effect.

Diethylthiocarbamate copper (CuEt), a metabolite of Disulfiram (DSF), has been considered a potential anti-cancer drug by inducing tumour cell death and activating the immune system. Previous research has provided evidence of the capacity of Cu to initiate oxidative damage and inflammatory responses. Mitogen-activated protein kinases (MAPKs) play a critical part in processes such as stress responses, differentiation, and apoptosis of cells. Kinases believed to have an essential role in these processes are p38 mitogen-activated protein kinase (p38 MAPK), extracellular signal-regulated protein kinase (ERK), and c-Jun N-terminal kinase (JNK). Specifically, ERK is believed to help regulate the production of NF-κB (fig.1) which was overexpressed in previous in vitro experiments with human cells treated with CuEt.
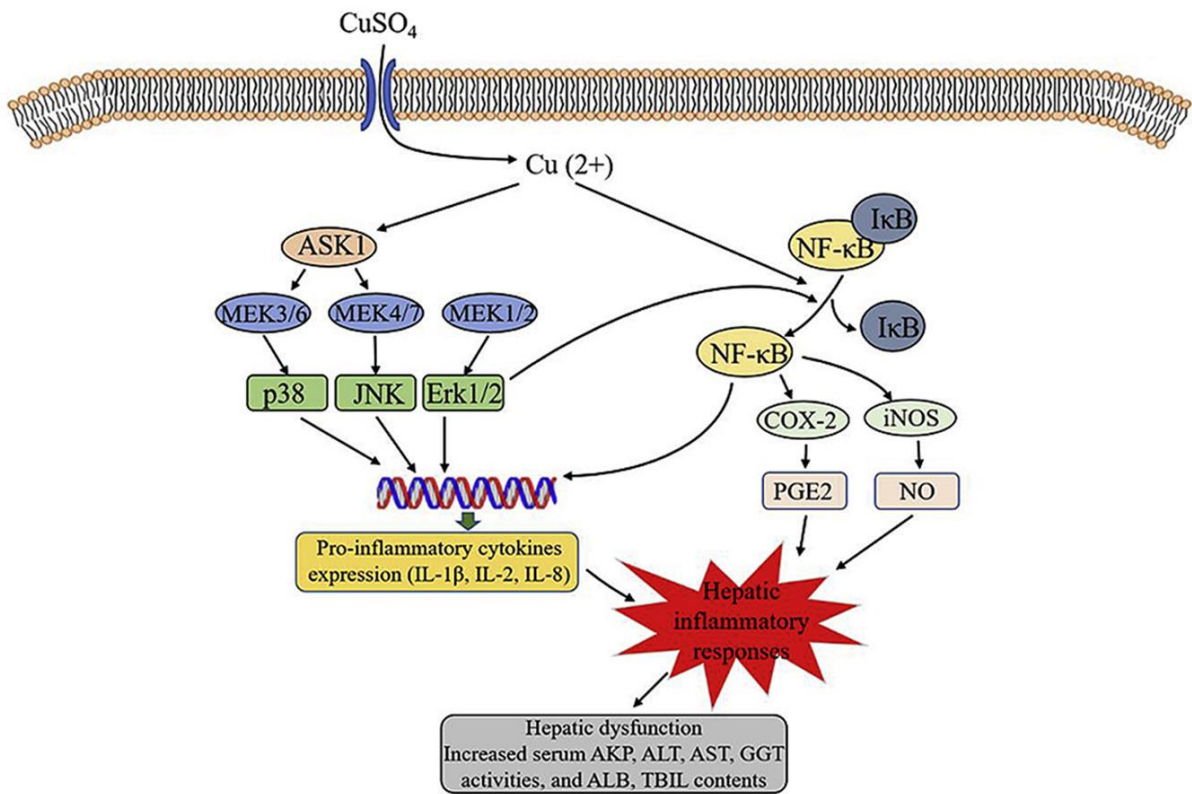
Fig. 4 - Schematic of Cu-induced hepatic inflammatory responses in mice. Cu can induce hepatic inflammatory responses via the activation of MAPKs and NF-κB pathways, which increase the expression levels of pro-inflammatory cytokines such as IL-1β, IL-2 and IL-8. (Liu, et al. Ecotoxicology and Environmental Safety 201 (2020) 11080610)

It is important to note that in this thesis, nanomolar concentrations of CuEt were used; therefore, the previously mentioned oxidative damage effect shouldn't play a role. As the aim of this thesis is to shed some light on the mechanisms responsible for the priming of the immune cells to be able to recognise and kill tumour cells, nanomolar concentrations were chosen to stimulate lymphocytes without killing or damaging them due to the previously mentioned oxidative damage effect of CuEt. In numerous research works, including my bachelor thesis, a dual effect of CuEt was shown when using nanomolar concentrations. This effect consists of both immune cells priming against the tumour cells and the tumour cells becoming more susceptible to immune cell-mediated apoptosis (V.Valentini, 2021). In the mouse tumour model, the effect of CuEt may depend on the strain. In a recent study, DSF has been found to bind to and activate the lymphocyte-specific kinase Lck, promoting Lck-mediated TCR signalling in CD8+ T-lymphocytes (Q.Wang *et al.*, 2022). This interaction is visualised in fig. 2 A, showing the upregulation of IL-2, IFNγ, and granzyme B. Splenic lymphocytes from C57BL6 and BALB/c mice differ in their cytotoxic response against tumours. We speculate that this effect occurs because the two different mice strains have different T-cell subpopulations, which CuEt can stimulate to another degree. This thesis aims to investigate this topic.
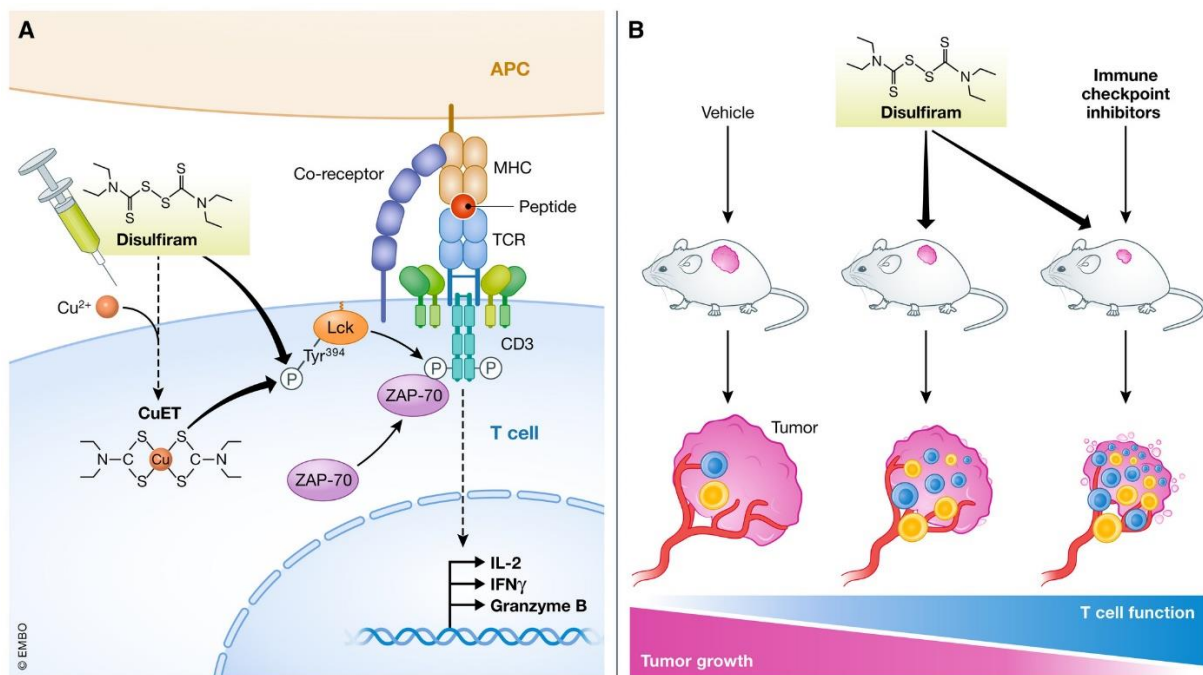
Fig. 5 – "The mechanisms of action of disulfiram and CuET on T cells -(A) In vitro, disulfiram and its reactive metabolite coupled with copper bind directly to Lck, setting in motion a chain of phosphorylation events leading to the activation of T cells with secretion of IL-2, IFNγ, and Granzyme B. (B) In vivo, disulfiram exerts antitumor effects by activating T cells in the tumour microenvironment, causing their local expansion and increasing local lytic activity. Combined with immune checkpoint inhibitors, the use is expected to yield synergistic protective antitumor effect." (M.Dosset *et* M.Zanetti, 2022)

2 Theoretical part

2.1 Disulfiram

Disulfiram (1-(Diethylthiocarbamoyldisulfanyl)-N, N-diethyl-methanethioamide) (Fig.3), also known as Antabuse is a drug used for several years now to treat alcohol use disorders. It is used for its aldehyde dehydrogenase (ALDH) inhibitory effects to discourage potential alcohol usage. In 1937 workers in a factory who were frequently exposed to DSF experienced flu-like symptoms after ingesting alcohol, such as a feeling of heat in the face, palpitations, and sometimes slight dyspnoea. If they consumed high amounts of alcohol, they often experienced nausea and vomiting. This effect led to the first clinical trials in 1948 where DSF was considered a potential anti-alcoholism treatment drug. In 1951 it was approved by the FDA as a drug for the treatment of alcoholism (Lu *et al.* 2021). Drug repurposing is an auspicious approach to finding treatments for diseases in already in-use drugs. It helps to reduce the time and cost of research and development of a treatment (Lu *et al.* 2021). Numerous studies have shown that DSF also has anti-cancer properties. Firstly, this was attributed to its ALDH inhibitory effect, but it has been proven DSF itself has no direct ALDH inhibitory effects. To assess the direct effect of disulfiram on ADH, Yourick JJ *et* Faiman M D (1991), blocked P450 cytochrome upon DSF administration. Liver ALDH function was unaffected, meaning DSF metabolites are responsible (Yourick JJ et Faiman MD, 1991). Some metabolites have been found to have an ALDH inhibitory function, such as S-methyl-N and N-diethylthiocarbamate-sulfoxide (Me-DTC-SO). This was also thought to be the metabolite responsible for the anti-cancer effects. This was disproven in a study by Skrott *et al.* in 2017 where the ALDH inhibitory function of Me-DTC-SO was confirmed, but its tumour-suppressing effects were disproven. Instead, the study identified a metabolite called CuEt (bis(diethyldithiocarbamate)–copper) (Fig.2) which didn't inhibit ALDH function. The study also identified the DSF tumour-suppressing effects target as NPL4, an adaptor protein of the p97/VCP segregase complex. The two previously mentioned disulfiram metabolites (Me-DTC-SO, CuEt) were tested for their ALDH inhibitory function and their tumour-suppressing effects in a later study also using other unrelated compounds like DEAB which have an ALDH inhibitory function. This study has proven that ALDH inhibition isn't the cause of the tumour-suppressing effect and identified CuEt as the metabolite responsible. (Skrott et al.,2019).
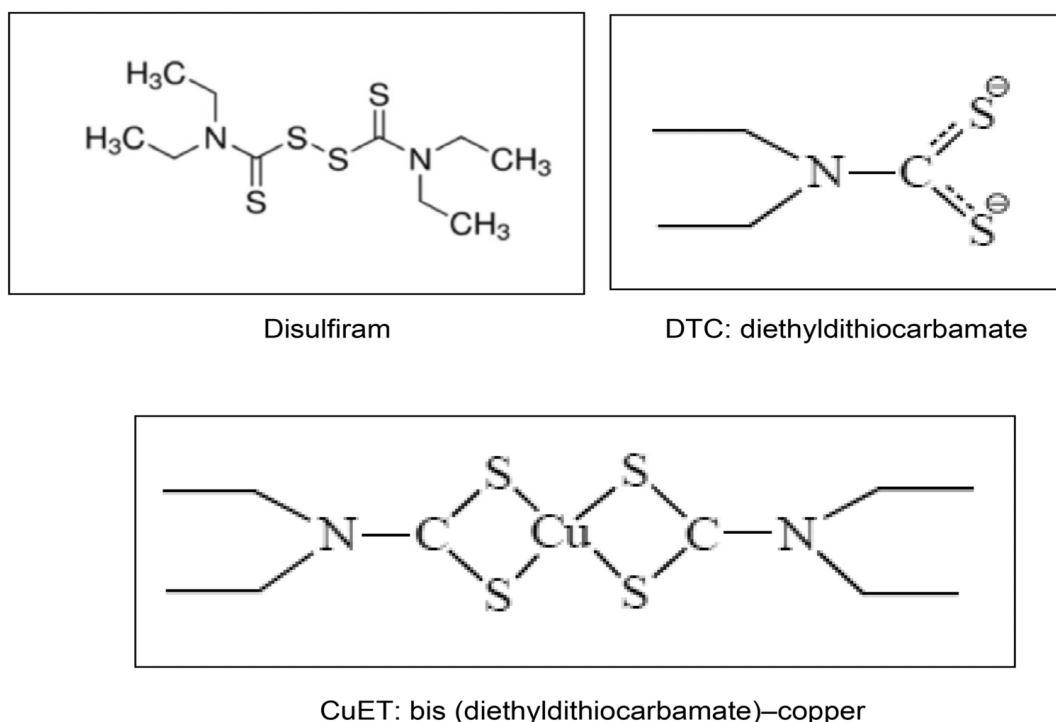
Disulfiram

DTC: diethyldithiocarbamate

CuET: bis (diethyldithiocarbamate)–copper

Fig. 6 - Structure of Disulfiram, DTC and CuET (Skrott et al. 2017)

Both DSF and its metabolite diethyldithiocarbamate (DDC) exhibit stability in basic environments but are prone to instability in acidic conditions. When consumed, over 99% of DSF rapidly converts to its corresponding thiol metabolite DDC within the stomach's acidic environment. Both forms are swiftly absorbed through the gastrointestinal mucosa into the portal circulation and accumulate in the liver, where rapid metabolism and degradation of both DSF and DDC occur. Due to its hydrophilic and polar nature, DDC readily undergoes reduction to diethylamine (DEA) and carbon disulfide (CS2). The reactive nature of CS2 enables it to interact with endogenous nucleophilic groups such as thiols, amino acids, and proteins, leading to carbonyl sulfide (COS) formation. This process can further result in the oxidation of COS into carbon dioxide and sulfur radicals, which permanently inhibit microsomal mono-oxygenases. Additionally, CS2 can participate in the re-synthesis of DDC by reacting with DEA in vivo, potentially explaining the prolonged intolerance to alcohol. Both DSF and DDC possess strong chelating abilities towards divalent transition metal ions, forming stable complexes. The metal complex, Cu(DDC)2, appears as a dark precipitate, exhibiting greater stability in acidic environments. The neutral and hydrophobic characteristics of Cu(DDC)2 facilitate its systemic absorption along the upper gastrointestinal tract. It is worth noting that the presence of an intact

thiol group in both DSF and DDC is crucial for their effective chelation of divalent transition metal ions. (V. Kannappan *et al.,* 2021)

A quite recent study Q.Wang *et al.* from 2022 showed that DSF enhances CD8+ cell responses against cancer by binding to the lymphocyte-specific protein tyrosine kinase (LCK), enhancing its activity. That study also showed that DSF induces the production of IL-2 and effector cytokines, promoting proliferation and metabolic reprogramming of CD8+ cells.

2.2 Tumour microenvironment

Solid tumours are surrounded by a heterogenous, complex microenvironment made up of many components which all directly or indirectly work to promote the survival of the tumour (N. Anderson *et* C.Simon, 2020). These components can be split into two main categories: acellular and cellular. The tumor microenvironment encompasses all signal molecules, secreted factors, extracellular matrix, infiltrating host and resident cells, and immune cells close to the tumour, influencing its growth and development (N. Anderson *et* C.Simon, 2020). During the early stages of tumor growth, a dynamic and reciprocal interplay emerges between cancer cells and the constituents of the tumor microenvironment, creating a symbiotic relationship that facilitates cancer cell survival, local invasion, and metastatic dissemination. In response to the adverse conditions of low oxygen and acidity within the microenvironment, the tumor microenvironment coordinates a range of mechanisms to promote angiogenesis, restoring the supply of oxygen and nutrients while eliminating metabolic waste. As a result, tumors become infiltrated by a diverse array of adaptive and innate immune cells capable of performing both pro- and anti-tumorigenic functions (N. Anderson *et* C. Simon, 2020).

Immune cells, mainly macrophages, T-cells, dendritic cells and natural killer cells (NK) infiltrate the tumour microenvironment and are needed for tumour suppression. The main problem is that myeloid-derived suppressor cells (MDSCs) negatively impact the function of immune cells and lead to the inhibition of activation of T-cells, NK cells and macrophages. These cells promote the growth of the tumour by allowing it to escape immune oversight (N. E. Sounni *et* A. Noel, 2013).

2.3 JAK-STAT pathway

The Janus kinase – signal transducer activator of transcription (JAK-STAT) pathway is considered a very evolutionarily conserved pathway. The pathway influences extracellular signals and molecules, primarily cytokines, on gene transcription and overall expression. This

effect depends on the activation of the receptor, which induces conformational changes. Consequently, the Janus kinase is recruited to the receptor, binds to it, and transmits the signal by phosphorylating the tyrosine residue. This, in turn, leads to the recruitment and phosphorylation of downstream molecules, such as STAT proteins. Some of the Different interactions of different JAKs and STATs is shown in fig. 4. Subsequently, these proteins form dimers and can translocate into the nucleus. Once inside the nucleus, they can influence transcription (J. O'Shea *et al.*, 2015), (C. Xue *et al.,* 2023).

The JAK-STAT pathway is crucial for the differentiation and development of immune cells by allowing these cells to respond to cytokines by modulating their nuclear transcription of different genes. Therefore, it is also important to upkeep the correct regulatory processes of the immune system. The JAK-STAT pathway's ability to generate a response on the nuclear level is also used in cell recognition. One such recognition is cancer cell recognition which IFNs and STAT1 and STAT2 signaling mainly mediate. Interestingly IL-6 STAT3 signaling is thought to enable immune escape of cancer cells by upregulating the differentiation of Th17 cells (J.J. O'Shea *et al*., 2013; C. Xue *et al.,* 2023)
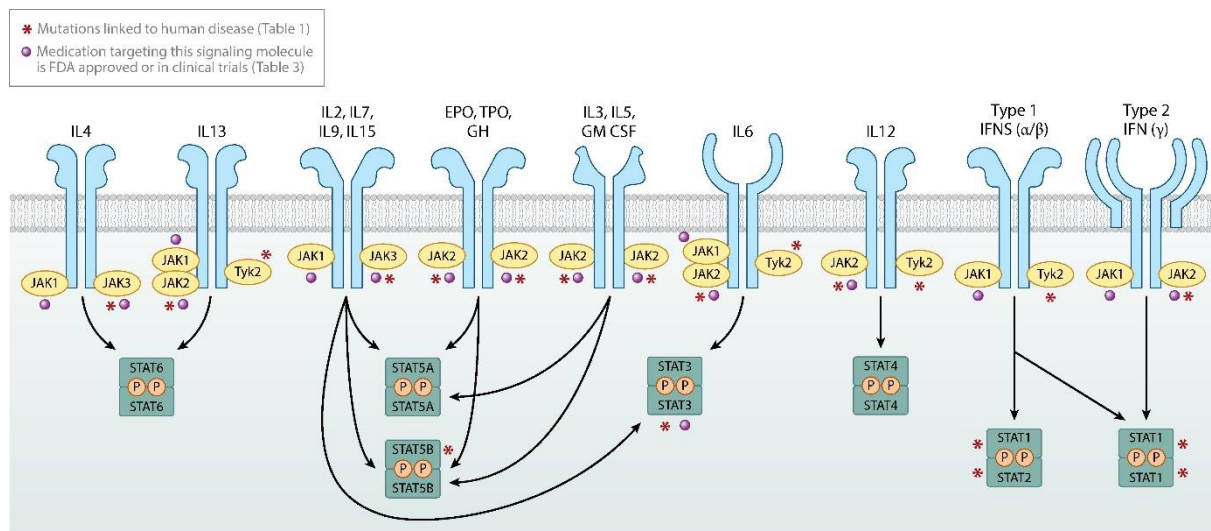
O'Shea JJ, et al. 2015.
Annu. Rev. Med. 66:311–28

Fig. 7 – An overview of different JAKs and their functions - "The four JAKs (JAK1, JAK2, JAK3, TYK2) are selectively bound to and therefore mediate signaling for various cytokine and hormone receptors. Different cytokines also have a propensity to activate certain STATs. Mutations in many of the genes encoding JAKs and STATs (indicated by an asterisk) have been linked to human disease. A large number of medications targeting JAKs and, to a lesser degree, STATs (indicated by a ·) are being developed and used to treat human disease"(J.J. O'Shea et al. 2015).

2.3.1 Janus kinases

The JAK family of non-receptor tyrosine kinases comprises four proteins: JAK1, JAK2, JAK3, and TYK2. Each of these kinases acts as an intracellular adaptor protein in cytokine signaling. JAK3 is primarily expressed in hematopoietic cells, whereas the other members exhibit widespread expression in various tissues. The JAK proteins consist of different domains, including FERM (Four point one, ezrin, radixin, and moesin), Src homology domain (SH2), pseudokinase, and kinase domains. The FERM domain consists of F1, F2, and F3 substructures and plays a role in JAK binding to receptors. The pseudokinase domain regulates the activity of the kinase domain, which is crucial for phosphorylating receptor tyrosine residues and subsequently phosphorylating downstream molecules. These domains are further divided into seven partitions, denoted as JH1–7. JH1 and JH2 are located at the C-terminal end, while JH3–7 are found at the N-terminal end. JH1 encodes a kinase that phosphorylates a critical component of the substrate's kinase domain, while JH2 acts as a pseudokinase domain that enhances the kinase function of JH1. JH3 and JH4 contribute to maintaining the stability of the kinase structure, while JH5, JH6, and JH7 facilitate JAK attachment to specific receptors. JAK activation is primarily triggered by cytokines such as interferons, interleukins, growth factors, and their corresponding receptors. The receptor-bound JAK is activated upon ligand-receptor binding, leading to receptor tyrosine phosphorylation. The four known members of the JAK family interact with specific cytokine receptors and recruit corresponding STATs (signal transducers and activators of transcription) to perform diverse biological functions. JAK1, JAK3, and TYK2 contribute to immune system development and regulation, while JAK2 primarily participates in hematopoiesis (C. Xue et al., 2023).

2.3.2 STAT proteins

STAT proteins were initially identified as latent cytoplasmic transcription factors, remaining in the cytoplasm until they translocate to the nucleus through JAK-mediated phosphorylation and dimerisation after cytokines activate them. Subsequently, these activated STAT dimers, once in the nucleus, can bind to specific DNA-recognition motifs known as gamma-activated sites (GAS) in the promoters of genes inducible by cytokines, leading to the activation of transcription (T. J. Mitchell *et* S. John, 2005). STAT1, STAT2, STAT3, STAT4, STAT5A, STAT5B and STAT6 form the STAT protein family. They all contain an N-terminal domain, a coil, a DNA-binding domain, an SH2 domain, a transcription activator domain, a connection

domain, and a helix domain (C. Xue et al., 2023). The structure of STAT1 binding to DNA is shown in fig. 5.
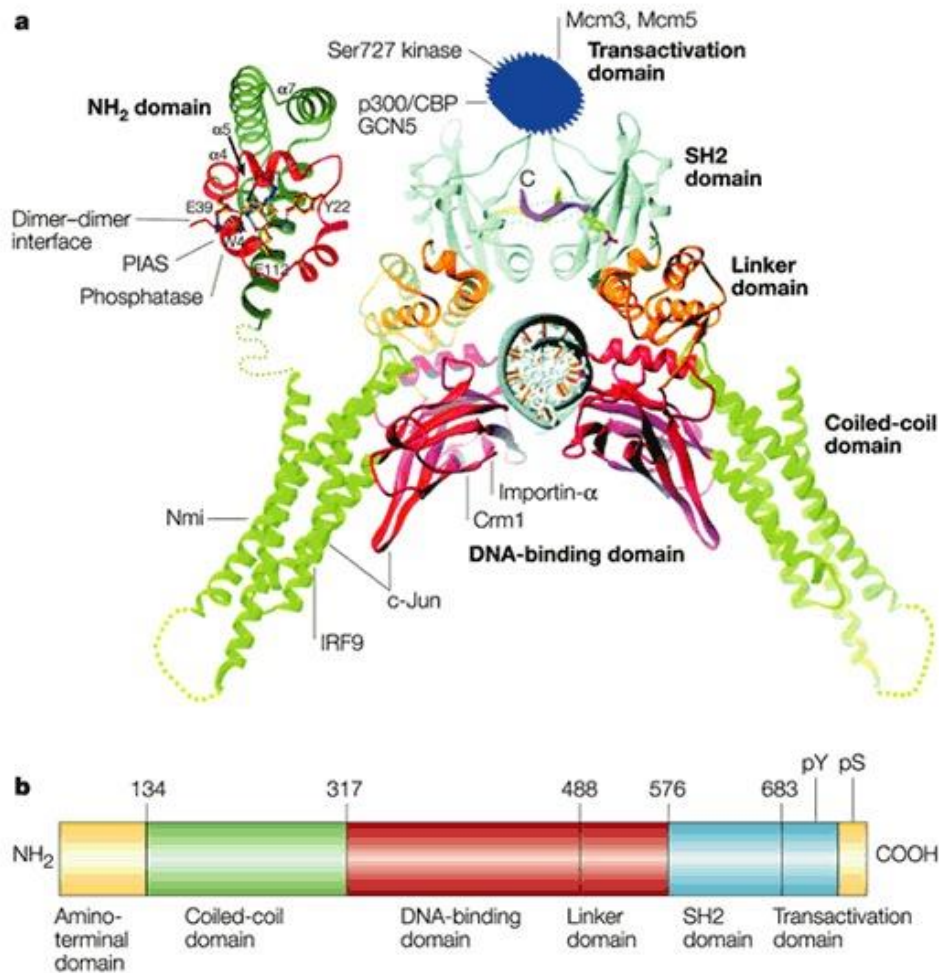
Fig. 8 – "STAT domain structure and protein binding sites.a | The core structure (amino acids 130–712) shows binding of a STAT1 dimer to DNA and the location of binding sites of various proteins in various domains. The amino-terminal structure, the placement of which in the intact structure is undefined, also interacts with various partners, as does the carboxy-terminal transactivation domain." "b | STAT structure. STAT, signal transducer and activator of transcription. SH2, Src-homology-2 domain." (D.Levy et Jr. J. E. Darnell, 2002)

The N-terminal domain and coil facilitate the formation of STAT dimers. As a regulator, the helix domain controls nuclear import and export processes. STATs, serving as transcription factors, bind DNA through their DNA-binding domain. It recognizes phosphorylated tyrosine residues on specific cytokine receptors, the SH2 domain plays a crucial role. Upon phosphorylation of the receptor tyrosine, cytosolic STATs are recruited to the activated

receptor. This leads to the phosphorylation of a STAT tyrosine residue, resulting in the formation of STAT dimers. As components of transcription factor complexes, these dimers enter the nucleus to promote the transcription of specific target genes. Once in the nucleus, STATs undergo dephosphorylation and are subsequently transported back to the cytoplasm. Among the members of the STAT family, STAT3 has a well-established role in transmitting signals from the plasma membrane to the nucleus (C. Xue et al., 2023). The structure of STAT3 while in a complex with DNA is shown in Fig. 6.

2.3.3 STAT3

STAT3 is a protein that is part of the STAT protein family. As previously mentioned, proteins from this family are each activated by a different cytokine receptor. They all seem to have high specificity in their signalling pathways. Studies with mice with one or more STAT proteins knocked out showed some relatively discrete changes in phenotype, allowing for assigning specific pathways to each STAT protein. This, however, couldn't be done with STAT3. The ablation of STAT3 leads to embryonic lethality, confirming the importance of STAT3 (D. E. Levy *et* C. Lee, 2002).

Structurally STAT3 is similar to other STAT proteins. Just like other STAT proteins STAT3 is phosphorylated on tyrosine by a Janus kinase. This phosphorylation is required for the dimerisation of STAT3, which then leads to it being able to translocate into the nucleus and bind to DNA to influence transcription. (D. E. Levy et C. Lee, 2002).
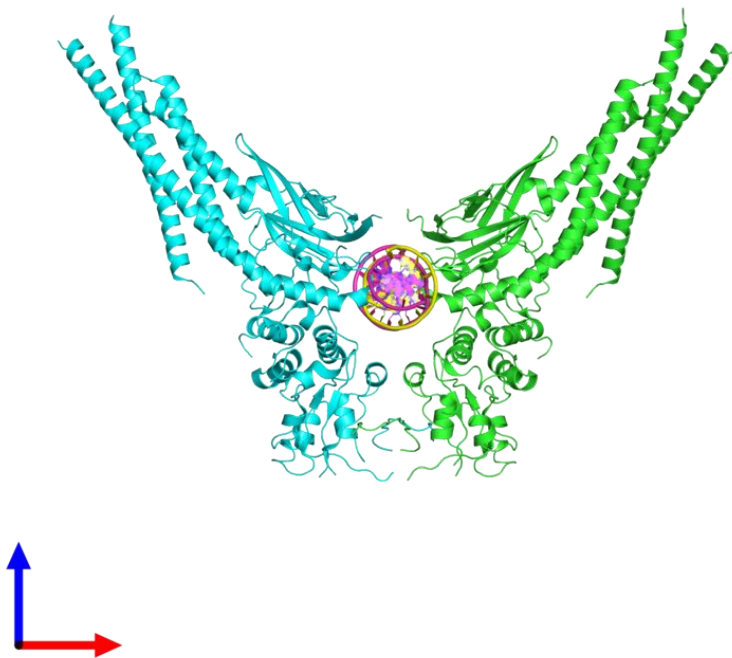
STAT3 deficiency is characterised by STAT3 hyper IgE syndrome (STAT-HIES). STAT-HIES is a primary immune deficiency which happens when the patient has a heterezygous dominant-negative pathogenic variant in STAT3 (A. P. Hsu *et al., 2010*). The symptoms are a rash usually in the newborn period, which evolves into an eczematoid dermatitis, recurrent staphylococcal skin boils, bacterial pneumonia, and mucocutaneous candidiasis. Interestingly, the increased frequency of lymphomas implies the important role STAT3 might play in cancer immunity (A. P. Hsu *et al., 2010*). Another interesting fact is the ability of T-reg cells to change into Th17 cells through the IL-6 STAT3 mediated pathway, which would suggest the possibility of lowering T-reg cell count in the tumour microenvironment while increasing Th17 cell counts resulting in lower immune evasion and higher possible IL-21 stimulation of effector cells. As previously mentioned, the complete absence of functional STAT3 leads to embryonic death (D. E. Levy *et* C. Lee, 2002).

2.4 NKG2D

As mentioned in the introduction NKG2D - natural killer group 2 member D (CD314) is a transmembrane receptor protein mainly expressed on the surface of NK and CD8+ cells. In CD8+ cells NKG2D when bound to a ligand acts as a co-stimulatory signal that amplifies and

enhances the cytotoxic reaction after TCR recognition. It binds to ligands such as MICA/B and UBLP proteins in humans and retinoic acid early inducible gene ε (Rae-1ε), MULT-1, and H60 in mice (A. Zloza *et al*., 2012, Y. Kim et al. 2020). The MICA ligands are usually not expressed in healthy cells but are associated with virally infected, heat shock or cancer-transformed cells (K. Prajapati *et al.* 2018). The presence of these antigens implies that a higher expression of NKG2D could lead to better immune recognition of tumour-transformed cells. In a study by Hu *et al.* in 2016, they found that by stimulating CD28 on CD8+ cells, the Lck kinase was constantly active, which led to it activating the Janus kinase (JAK), which in turn mediated the phosphorylation and the dimerisation of STAT3, leading to a higher NKG2D expression. This interaction is relevant as a previously mentioned study by Q.Wang *et al.* from 2022 showed that DSF binds directly to Cys20/Cys23 residues of Lck, enhancing its tyrosine 394 phosphorylation which helps the promotion of its activity in CD8+ cells, which when put together with the findings of Hu *et al.* from 2016 would point to a possible similar mechanism.

2.5 Perforin

Perforin, a glycoprotein, plays a crucial role in creating openings in the cell membranes of target cells. It has the remarkable ability to combine and form channels within the membrane of these specific cells. The primary sources of perforin are natural killer (NK) cells and CD8-positive T-cells. However, even CD4-positive T-cells can express a small amount of perforin under specific circumstances when the typical cytotoxicity is impractical or disrupted. The polymerised perforin molecules establish channels allowing free and non-selective transport of ions, water, small molecules, and enzymes. As a result, these channels disrupt the protective barrier of the cell membrane and compromise the integrity of the target cell. Perforin is classified as a glycoprotein weighing around 60-70 kDa, comprising 555 amino acids. A single perforin molecule consists of four distinct domains. These domains include two specific ones (known as the N-terminal and C-terminal domains), which are closely associated with the biological functions of perforin. The remaining two domains, located within the molecule's centre, bear a 20% similarity to analogous domains found in complement molecules such as C6, C7, C8, and C9. Within one of these similar domains, a sequence facilitates the formation of two β-sheets and one α-helix structure. This specific hydrophobic domain can integrate into the lipid membrane of the target cell. Additionally, the perforin molecule contains a cysteine-rich domain that shares homology with the low-density lipoprotein (LDL) receptor type B and the epithelial growth factor (EGF) precursor. The N-terminal domain of perforin possesses a

binding site for Ca2+ ions, which is intricately linked to its biological function (I. Osińska *et al.*, 2014)

Perforin along with granzyme B have a very important role in cytotoxicity of CD8+ and NK cells, as both of them use the release of perforin and granzyme B to destroy target cells by perforating the cell membrane and inducing the osmotic lysis of the target cell. Perforin function can be inhibited in low pH and high concentration on Ca ions or by the activity of protein S (I. Osińska *et al.*, 2014).

2.6 NF-κB

In 1986, David Baltimore's research group made an important discovery by identifying the NF-κB family as a transcription factor specific to B cells. This family comprises five DNA-binding proteins that can form a wide range of homodimers and heterodimers. These events play a pivotal role in regulating both innate and adaptive immune responses induced by a multitude of stimuli such as cytokines, UV stress free radicals and more, the NF-κB proteins promote inflammatory response after translocating to the nucleus and serve as crucial modulators of transcription in stress response. They have the capacity to accelerate cell proliferation, inhibit apoptosis, stimulate cell migration and invasion, and induce angiogenesis and metastasis (K. Taniguchi *et* M. Karin, 2018).

The activation of target genes by NF-κB dimers, which occurs through binding to specific DNA-binding sites, often requires the collaboration of other transcription factors. Notably, members of the signal transducer and activator of transcription (STAT) family, activator protein 1 (AP1) family, and interferon regulatory factors (IRFs) can assist in facilitating this process. (K. Taniguchi *et* M. Karin, 2018).

In my bachelor thesis I confirmed that NF-κB is crucial to CuEt's anti-cancer effect by using NF-κB inhibitors. When NF-κB inhibitors were used, cytotoxicity against HT29 and HCT116 cell lines was statistically significantly lower than the negative control.

As mentioned by K. Taniguchi *et* M. Karin in their article from 2018, NF-κB is very often associated with cancer as its signalling abilities can allow for angiogenesis proliferation and even immune escape of the tumour among other things. But NF-κB is also responsible for granzyme B and perforin gene expression in NK and CD8+ cells through an IL-2 mediated signalisation pathway (C. Huang *et al.*, 2006; J. Zhou *et al.*, 2002).

2.7 ERK1/2

ERK1 and ERK2, a pair of protein-serine/threonine kinases, are interconnected within the Ras-Raf-MEK-ERK pathway responsible for transmitting signals into the cell. This intricate pathway governs a diverse range of biological functions, such as cell adhesion, progression through the cell cycle, migration of cells, survival of cells, differentiation, metabolic regulation, proliferation, and transcriptional activities (R. Roskoski Jr., 2012). In a research paper published in 2004 by Z. J. Tian and W. An, ERK1/2 was found to negatively modulate STAT3 tyrosine phosphorylation in HSS-transfected HepG2 cells by phosphorylation of serine 727 on STAT3. This was proven by introducing STAT3, which was mutated in serine 727. The mutated STAT3 didn't show lower tyrosine phosphorylation than control. In stark contrast to this a study by N. Queisser *et al.* from 2017 showed that aldosterone treated rat kidneys had an increased phosphorylation of both ERK1/2 and STAT3, while also claiming that ERK1/2 was responsible for the higher rate of activated STAT3. Both of these studies show that ERK1/2 clearly modulates the phosphorylation of STAT3 in some way. ERK1/2 is also known to induce the degradation of IκBα, an NF-κB inhibitor.

As mentioned in the introduction the src family kinase p56^{lck} (Lck) is bound by CuEt resulting in an enhancement of TCR mediated signalling by CD8+ T-cells (Q.Wang *et al.*, 2022). Lck has also been shown to influence the activation threshold in naïve T-cells by mobilising Ca^{2+} ions and activating the ERK pathway (M. Lovatt *et al.*, 2006).

2.8 Hypothesis

Based on the previous research, I have concluded that my final hypothesis on the possible mechanism involved in the activation of T-cells with nanomolar concentrations of CuEt goes as follows.

CuEt activates CD8 and NK lck priming the cells and activates the ERK1/2 pathway inducing an increase in active NFkB (p65 dimer particularly). The Lck kinase would then also activate the JAK/STAT pathway, leading to the tyrosine phosphorylation and dimerisation of STAT3. This priming effect induces the transcription and expression of NKG2D, granzyme, and perforin production. Autocrine IL-2 costimulates the primed cells rendering them more cytotoxic. (M. Dosset et M. Zanetti, 2022; Q.Wang et al., 2022). This possible mechanism is showcased in fig. 7.
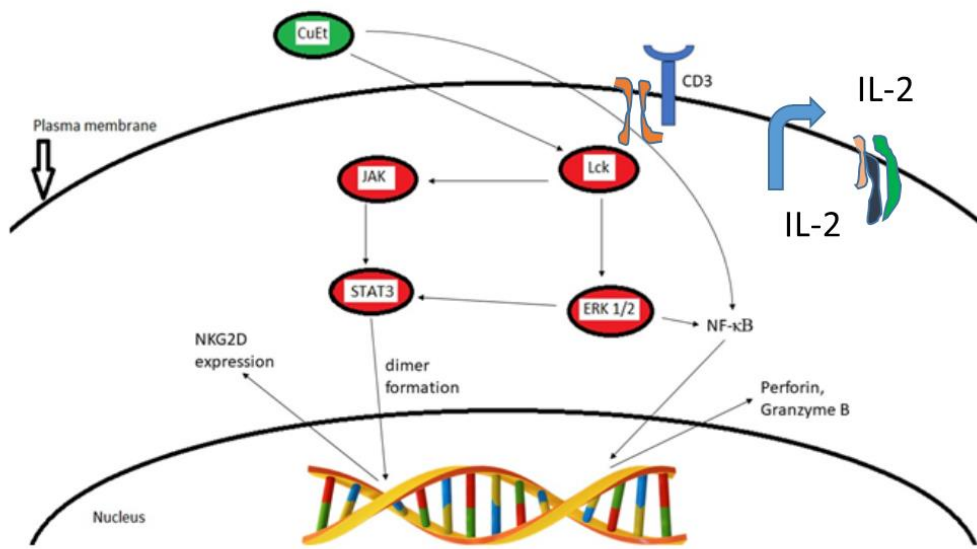
Fig. 10 - The possible mechanism of CuEt mediated CD8+ T-cell cytotoxicity increase

3 Materials and Methods

3.1 Materials

3.1.1 Mice strains

- BALB/c

- C57BL/6

3.1.2 Chemicals

- BD Cytofix/Cytoperm™ Fixation/Permeabilization Kit (CAT. NO.: 554714)

- 1-Butanol (Penta s.r.o., Czech Republic, CAT. NO.: 22120-11000)

- Bovine Serum Albumin (Sigma-Aldrich, USA, CAT. NO.: A7906)

- Bromphenol blue (Unknown company, Czechoslovakia)

- CuEt 10mM

- DTT (dithiothreitol) (Thermo Scientific™, USA, CAT. NO.: R0862)

- Ethanol (96%) (Penta s.r.o., Czech Republic, CAT. NO.: 70390-11001)

- Glycerol (Sigma-Aldrich, USA, CAT. NO.: G5516)

- Immobilon Forte Western HRP substrate (EMD Millipore Corporation, USA, CAT. NO.: WBLUF0500)

- Gibco™ PBS (phosphate buffered saline) (Thermo Fisher Scientific, CAT. NO.: 10010015)

- MojoSort™ Mouse CD4 T Cell Isolation Kit (BioLegend®, Inc., CAT. NO.: 480033)

- MojoSort™ Mouse CD8 T Cell Isolation Kit (BioLegend®, Inc., CAT. NO.: 480035)

- Pierce™ Bovine Serum Albumin Standard Pre-Diluted Set (Thermo Scientific™, USA, CAT. NO.: 23208)

- Phosphatase Inhibitor Cocktail Tablets PhosSTOP EASYpack (Roche Diagnostics Deutschland GmbH, Germany, CAT. NO.: 4906837001)

- Protease Inhibitor Cocktail Tablets cOmplete Tablets EASYpack (Roche Diagnostics Deutschland GmbH, Germany, CAT. NO.: 04693116001)

- Spectra™ Multicolor Broad Range Protein Ladder (Thermo Scientific™, USA, CAT. NO.: 26623)

- Sodium Dodecyl Sulfate (Sigma-Aldrich, USA, Batch no.: STBD5191V)

- Penicillin-Streptomycin (Sigma Aldrich, USA, CAT. NO.: P4458)

- Trizma® hydrochloride (Sigma-Aldrich, USA, CAT. NO.: T3253)

- Tween-20 (Sigma-Aldrich, USA, CAT. NO.: P2287)

3.1.3 Stock solutions

- Pierce™ BCA Protein Assay Reagent A (Thermo Scientific™, USA, CAT. NO.: 23223)

- Pierce™ BCA Protein Assay Reagent B (Thermo Scientific™, USA, CAT. NO.: 23224)

- RPMI 1640 Complete Medium, with 2mM L-Glut and 10% FBS (Sigma-Aldrich, USA, CAT. NO.: SLM-240)

- RIPA Lysis and Extraction Buffer (Thermo Scientific™, USA, CAT. NO.: 89901)

- TGX Stain-Free™ FastCast™ Acrylamide Kit, 12% (Bio-Rad Laboratories, Inc., USA, CAT. NO.: 1610185)

- Trans-Blot Turbo 5x Transfer Buffer (Bio-Rad Laboratories, Inc., USA, CAT. NO.: 10026938)

- 10x Tris/Glycine/SDS (Bio-Rad Laboratories, Inc., USA, CAT. NO.: 1610772)

- Western Blot Stripping Buffer (Santa Cruz Biotechnology, Inc., USA, CAT. NO.: sc-281698)

3.1.4 Laboratory equipment

- Bürker cell counting chamber (Paul Marienfeld GmbH & Co. KG; CAT. NO.: 0640210)

- ChemiDoc MP Imaging System (Bio-Rad Laboratories, Inc., USA)

- Dry block thermostat Bio TDB-100 (Biosan, Latvia)

- Nunc™ 15mL and 50mL Conical Sterile Polypropylene Centrifuge Tubes (Thermo Scientific™, USA; CAT. NO.: 339650)

- Hybridisation oven Techne Hybridizer HB-1D (Bibby Scientific Ld., United Kingdom)

- Gel Electrophoresis Mini-PROTEAN Tetra Handcast Systems (Bio-Rad Laboratories, Inc., USA)

- MilliQ® Ultrapure Water Systems (Merck KGaA, Germany)

- Rotina 420 R Centrifuge (Andreas Hettich GmbH & Co. KG, Germany)

- Spectrophotometer EnSpire Multimode Plate Reader (PerkinElmer, Inc., USA)

- Trans-Blot Turbo RTA Mini 0.2 μm Nitrocellulose Transfer Kit (Bio-Rad Laboratories, Inc., USA, CAT. NO.: 1704270)

- Trans-Blot Turbo Transfer System (Bio-Rad Laboratories, Inc., USA)

- Ultrasonic cleaner Sonorex Digitec DT (BANDELIN electronic GmbH & Co. KG, Germany)

3.1.5 Software

- Image Lab 6.1 Software (Bio-Rad Laboratories, Inc., USA)

- Graph Pad Prism (version 9.5.1)

- Microsoft Excel (365 version)

- Gel Quant

3.1.6 Working solutions preparation

1x TGS (1 l)

- 100 ml 10x Tris/Glycine/SDS

- 900 ml distilled H2O

5x SDS Loading buffer (pH = 6.8)

- 250 mM TRIS-HCl

- 0.5 M Dithiothreitol (DTT)

- 30% glycerol

- 10% sodium dodecyl sulphate (SDS)

- 0.06% bromphenol blue (Sigma-Aldrich, USA, CAT. NO.: 318744)

Transfer buffer (1 l)

- 600 ml MilliQ water

- 200 ml 5x Trans-Blot Turbo Buffer

- 200 ml 96% ethanol

10x TBS (1 l; pH = 7.6)

- 24.2 g TRIS base (Merck kGaA Germany)

- 80 g NaCl

- Distilled H2O

1x TBS-T (1 l)

- 100 ml 10x TBS

- 900 ml distilled H2O

- 1 ml Tween-20

5% Bovine Serum Albumin solution (100 ml)

- 5 g Bovine Serum Albumin

- 100 ml 1x TBS-T

3.1.7 Antibodies

- PE anti-mouse CD314 (NKG2D) Antibody (BioLegend®, Inc., CAT. NO.: 115606)

- APC anti-mouse Perforin Antibody (BioLegend®, Inc., CAT. NO.: 154304)

- Primary antibody p44/42 MAPK (Erk1/2) Antibody (Cell Signaling Technology, USA, CAT. NO.: 9102), dilution 1:1000 in 5% BSA

- Primary antibody Purified anti-ERK1/2 Phospho (Thr202/Tyr204) Antibody (BioLegend, Inc., USA, CAT. NO.: 369501), dilution 1:2000 in 5% BSA

- Secondary antibody Anti-Mouse IgG (whole molecule)–Peroxidase antibody produced in goat (Sigma-Aldrich, Cat. #A4416-1ML), dilution 1:10000 in 5% BSA

- Secondary antibody Anti-Rabbit IgG (whole molecule)–Peroxidase antibody produced in goat (Sigma-Aldrich, USA, CAT. NO.: A0545), dilution 1:10000 in 5% BSA

3.2 Methods

3.2.1 Spleen acquisition

Spleens from BALB/c and CD57BL/6 were obtained from the animal facility of the Institute of Molecular and Translational Medicine in Olomouc (IMTM) Hněvotínská 1333/5, 779 00 Olomouc, Czech Republic.

3.2.2 Splenocyte isolation

The spleen was put in a Petri dish containing PBS. Using a syringe with a needle, the spleen was pierced and injected with PBS, releasing some cells from the spleen. After the syringe was emptied, some of the PBS in the Petri dish was taken with the syringe and reinjected into the spleen. This was repeated until the spleen lost coloration and the PBS in the Petri dish was full of cells. The spleens were taken out of the Petri dish using tweezers, and the PBS with the released cells was transferred to a Falcon 15 ml tube. The sample was centrifuged at 1200 RPM for 10 minutes at 37 °C. The supernatant was carefully removed, and the pellet was resuspended in 5 ml PBS. Cells were counted with a Bürker cell counting chamber and adjusted to 10 million cells per 100 µl of PBS.

3.2.3 Separation of CD4+ and CD8+ cells

Separation was done using MojoSort™ Mouse CD8 T Cell Isolation Kit and MojoSort™ Mouse CD4 T Cell Isolation Kit. PBS was used as a buffer. 10 µl of the biotin antibody cocktail was added to the 100 µl samples in microtubes which were then put on ice. After 15 minutes, the samples had 10 µl of streptavidin nanobeads added and left on ice for another 15 minutes. Then, the samples were put into a stand with a magnet to one side, and the solution that didn't stick to the wall to which the magnet was next was carefully removed. The samples were washed with PBS 2x by mixing 200 µl of PBS and then using the magnet to retain the nanobead-marked cells in the tube while carefully removing the PBS using a pipette. After this the PBS was removed once more, and either 250 µl of RPMI or 1nM CuEt in RPMI solution or 10 nM CuEt in RPMI solution or 0,03% hydrogen peroxide in PBS solution was added. Samples were

then incubated at 37 °C for 10 minutes, then washed 2x using PBS and then frozen in -70 °C until protein extraction.

3.2.4 Protein extraction

The samples were centrifuged at 3000 RPM for 10 minutes at 4 °C. The supernatant was carefully removed. The sample pellets were mixed with RIPA solution (Thermo Scientific™) with phosphatase and protease inhibitors (30-40 µl each) and incubated on ice for 30 minutes. The samples were put in the ultrasonic sonicator bath for 2 minutes at temperature up to 10 °C. The samples were centrifuged at 12 000 RPM for 25 minutes at 4 °C. The supernatants were collected and used for protein quantification by BCA assay.

3.2.5 Protein quantification – BCA assay (Thermo Scientific™)

For protein quantification, a 96-well plastic plate was used. RIPA solution (Thermo Scientific™) served as blank, bovine serum albumin standard pre-diluted set (125, 250, 500, 750, 1000, 1500 and 2000 µg/ml) served as standards. The samples were diluted 3x in the wells with MilliQ water. Reagent solutions A and B were mixed (50:1), and 200 µl was added into each well for the reaction. The plate was incubated in a hybridisation oven for 30 minutes at 37 °C. The plate was loaded in a spectrophotometer and was measured at the wavelength of 562 nm.

3.2.6 Sample Preparation for SDS-PAGE

The protein samples were diluted to contain 30 µg of total protein per well. After dilution, 6x Laemmli buffer was added to each sample. The samples were denatured in the heating block for 5 minutes at 95 °C.

3.2.7 SDS-PAGE

The electrophoresis chamber was assembled. The 12% polyacrylamide gels (resolving and stacking gels, 1.5 mm thick) were prepared according to the instructions provided by the kit manufacturer. The electrophoresis chamber was placed in the electrophoresis cell, 1x TGS buffer was added, and samples were loaded into corresponding wells (30 µg of total proteins per well). The electrophoresis conditions were 80 V for 30 minutes, then 120 V until the dye front reached the bottom.

3.2.8 Semi-dry Western Blotting

The semi-dry western blotting was done according to instructions provided by BioRad Trans-Blot® Turbo™ Transfer System. The filter papers were soaked in a transfer buffer. The semi-dry western blot sandwich was assembled according to the manual sheet provided by the manufacturer. The preprogrammed protocol for 1.5 mm gels was selected with a blotting time of 10 minutes. After the blotting, the nitrocellulose membranes were stained with Ponceau S stain to confirm the successful transfer.

3.2.9 Immunodetection

The stained nitrocellulose membranes were washed in distilled water or 1x TBS-T buffer until clean. The membranes were then blocked in 5% Bovine Serum Albumin solution (BSA) for 1 hour. The primary antibody anti-ERK1/2 Phospho was diluted in 5% BSA. The membranes were incubated overnight in a primary antibody on the roller at 4 °C. After incubation, the membranes were washed 3x for 5 minutes each wash in 1x TBS-T buffer. The membranes were incubated in a secondary anti-mouse antibody conjugated with horseradish peroxidase (HRP) for 1 hour at room temperature. After incubation, the membranes were washed 3x for 5 minutes each wash in 1x TBS-T buffer. The membranes were then imaged with Biorad ChemiDoc™ MP Imaging System. Before imaging, the membranes were incubated in Immobilon® Forte Western HRP Substrate for 1.5 minutes in the dark. The imaging was processed with ImageLab software. After imaging, the membranes were washed in 1x TBS-T buffer, stripped in Western Blot Stripping Buffer for 10 minutes, and washed 2x for 5 minutes each wash in 1x TBS-T buffer. The primary antibody anti-p44/42 (ERK1/2) was diluted in 5% BSA. The membranes were incubated overnight in the diluted primary antibody on the roller at 4 °C. After incubation; the membranes were washed 3x for 5 minutes each wash in 1x TBS-T buffer. The membranes were then incubated in diluted secondary anti-rabbit antibody conjugated with horseradish peroxisade (HRP) for 1 hour at room temperature. After incubation, the membranes were imaged with Biorad ChemiDoc™ MP Imaging System as described previously above.

3.2.10 Band intensity quantification

The membranes' bands corresponding with 42 and 44 kDa were analysed and quantified with Gel Quant. The data was then evaluated with Microsoft Excel (365 version), and the graphs were generated using Graph Pad Prism 9 (version 9.5.1).

3.2.11 Flow cytometry staining

Splenocytes isolated in the same way as described in section 3.2.2 were incubated with RPMI medium or 1 nM or 10 nM CuEt for 18 hours. Then BD (Becton Dickinson) Cytofix/Cytoperm™ Fixation/Permeabilization Kit was used following the manual included in the kit to fixate the cells. The cells were then stained with PE marked anti-mouse CD314 (NKG2D) Antibody from BioLegend. For perforin, the cells were permeabilised and fixed with the BD (Becton Dickinson) Cytofix/Cytoperm™ Fixation/Permeabilization Kit and intracellular staining by APC anti-mouse Perforin Antibody from BioLegend was performed following the manual. Then flow cytometry was performed and the results were evaluated in Graph Pad Prism 9.

4 Results

The ERK pathway has been confirmed as an important pathway to study by other 2 assays performed on different pathways in the same laboratory I worked in.

The bands that correspond with 42 and 44 kDa on blotting membranes are shown in fig. 8,9 for BALB/c and in fig. 10,11 for C57BL6. These bands signals were quantified in Gel Quant as previously mentioned in materials and methods and graphs were made out of the gathered data. The first set of graphs (number 1-8) shows the percentage of total ERK detected that was phosphorylated. Green graphs (1,2,5,6) show BALB/c mice samples, while pink graphs (3,4,7,8) show C57BL6 mice samples. It is clear from these graphs that CD8+ cells, when treated with 1 or 10 nM CuEt exhibit a higher phosphorylation of ERK 1 (44 kDa) no matter the strain of mice. The ERK 2 (42 kDa) phosphorylation in CD8+ cells seems only to have increased in C57BL6 mice. However, it might be inconclusive as in graph 1 positive control showed lower phosphorylation of ERK 2 than control. CD4+ cells on the other hand, show the same and, in some cases, even lower phosphorylation than control. For example, ERK 2 in CD4+ cells shows lower phosphorylation even when treated with 0,03% H_2O_2 (positive control) in BALB/c (graph 5). However, This is not the case with ERK 2 in C57BL6 (graph 7) where positive control is slightly more phosphorylated than control. The amount of phosphorylation defined in percentage compared to control in both CD8+ and CD4+ treated is showcased in graphs number 9 – 12 for each strain and ERK separately. In these graphs, 100% means no change from control, while a lower or higher percentage shows a decrease or increase.
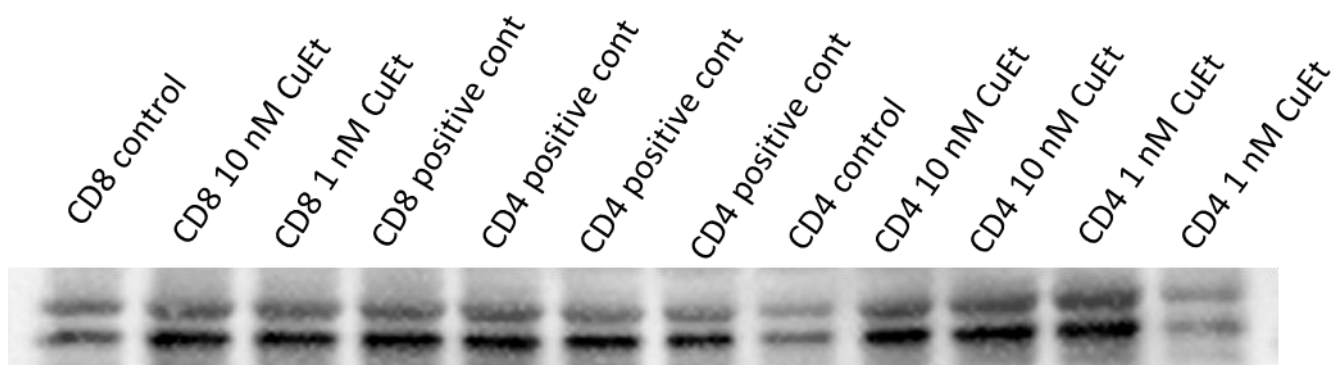

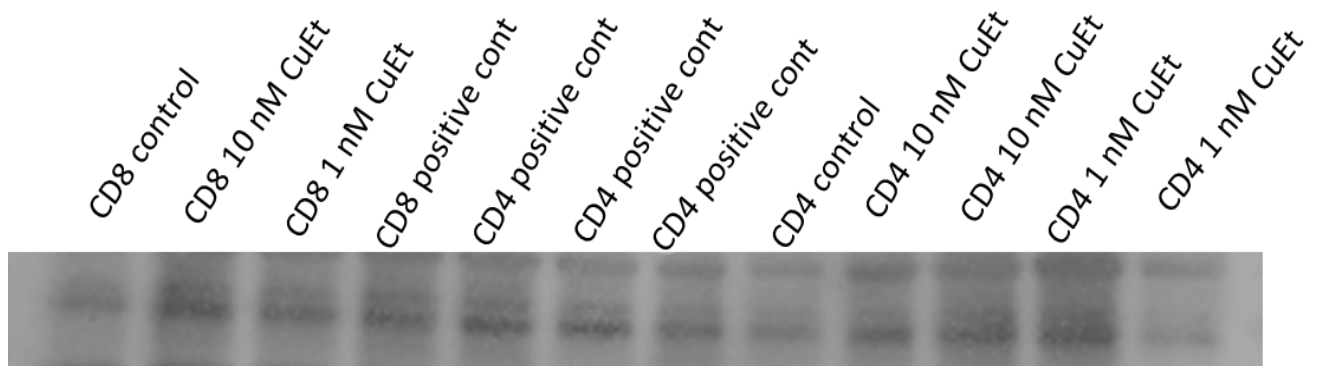*Fig. 11 - Blotting membrane with imuno-detected ERK 1/2 (42 and 44 kDa) BALB/c*

Fig. 12 - Blotting membrane with imuno-detected p-ERK 1/2 (42 and 44 kDa) BALB/c
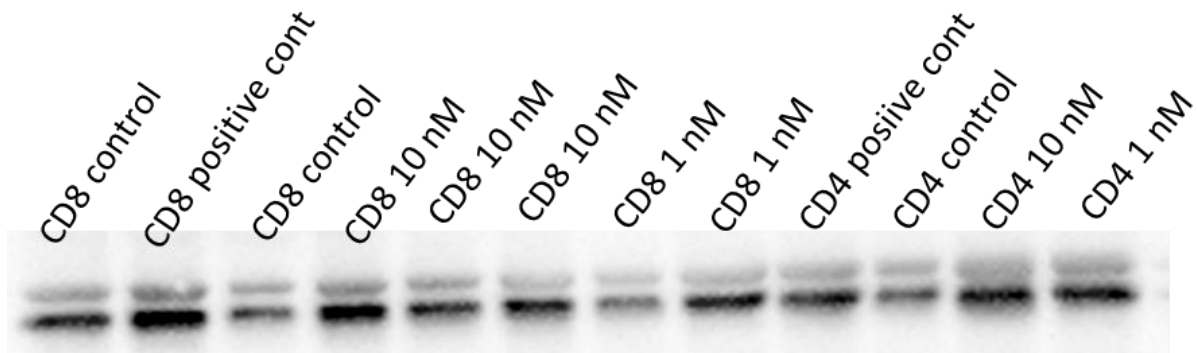

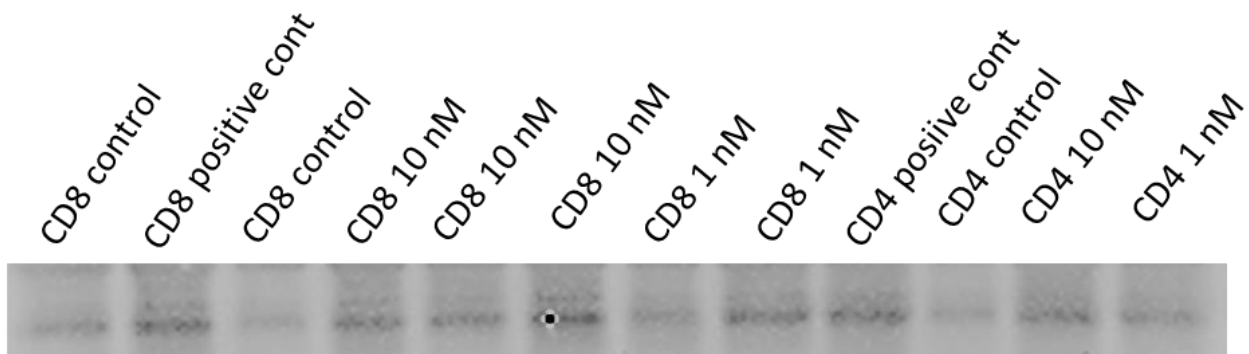*Fig. 13 - Blotting membrane with imuno-detected ERK 1/2 (42 and 44 kDa) C57BL6*
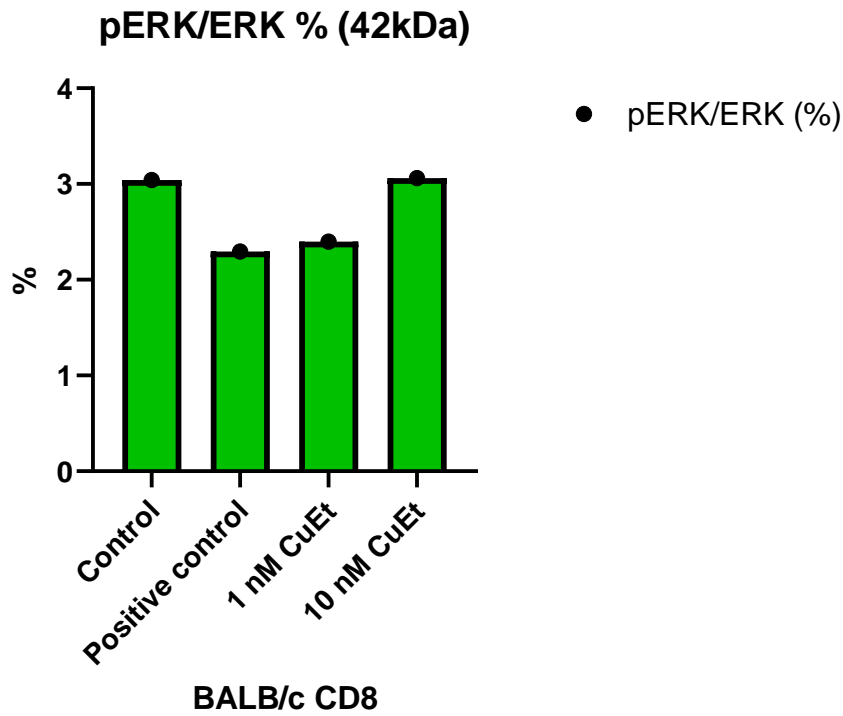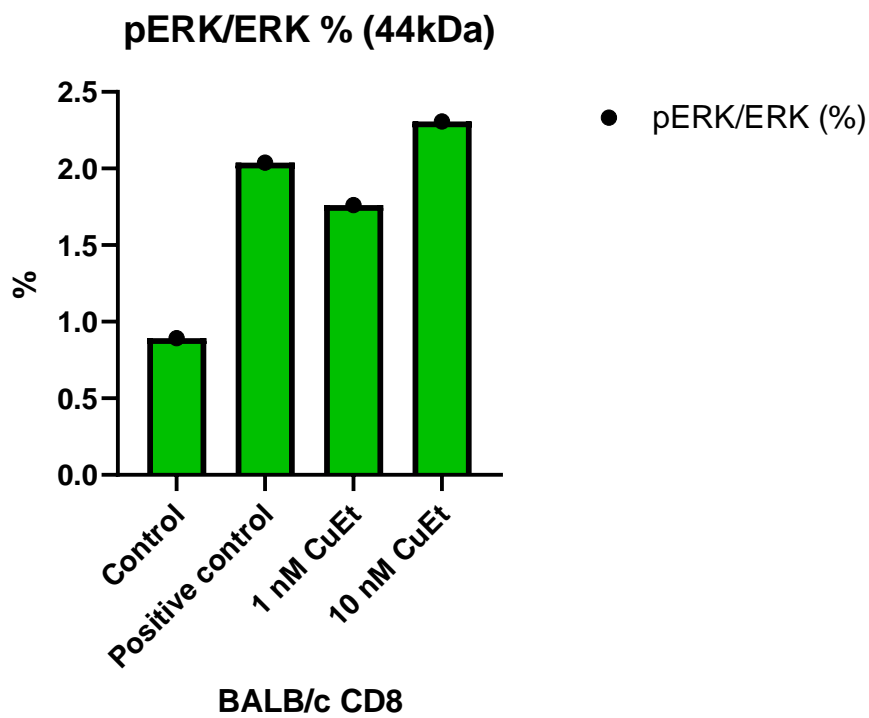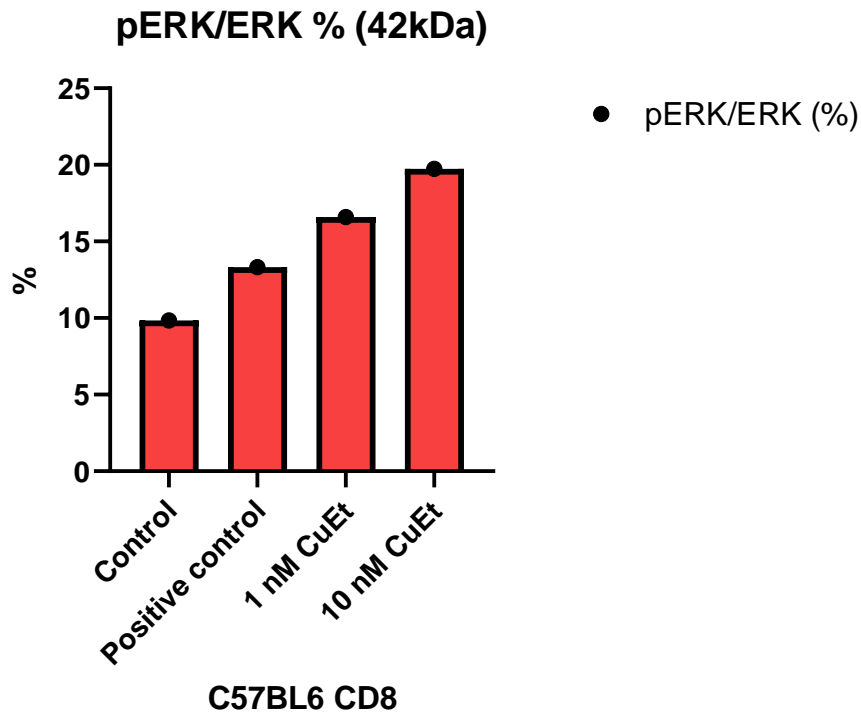

Fig. 14 - Blotting membrane with imuno-detected p-ERK 1/2 (42 and 44 kDa) C57BL6

pERK/ERK % (42kDa)

Graph 1 - Percentage quantity of phosphorylated ERK 2 compared to total ERK 2 detected in BALB/c CD8+ T-cells.

pERK/ERK % (44kDa)

Graph 2 - Percentage quantity of phosphorylated ERK 1 compared to total ERK 1 detected in BALB/c CD8+ T-cells.

pERK/ERK % (42kDa)

● pERK/ERK (%)

C57BL6 CD8

Graph 3 - Percentage quantity of phosphorylated ERK 2 compared to total ERK 2 detected in C57BL6 CD8+ T-cells.

pERK/ERK % (44kDa)

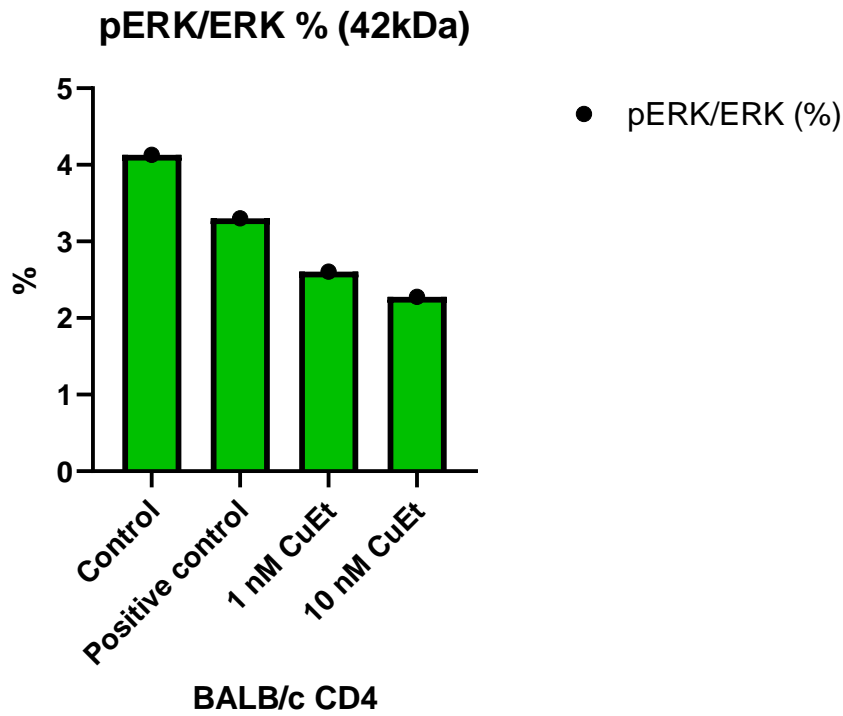● pERK/ERK (%)
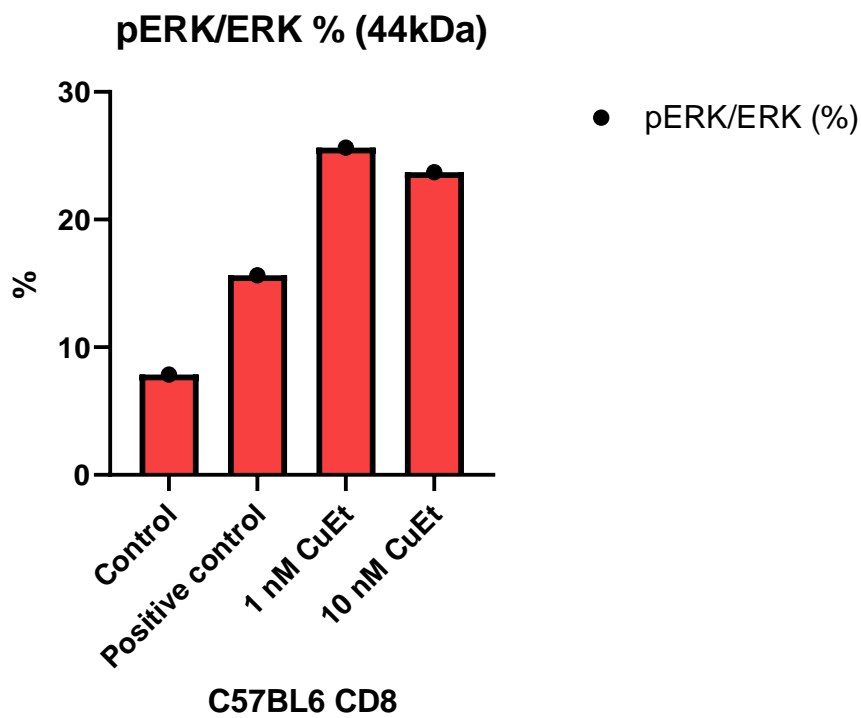
C57BL6 CD8

Graph 4 - Percentage quantity of phosphorylated ERK 1 compared to total ERK 1 detected in C57BL6 CD8+ T-cells.

Graph 5 - Percentage quantity of phosphorylated ERK 2 compared to total ERK 2 detected in BALB/c CD4+ T-cells.

Graph 6 - Percentage quantity of phosphorylated ERK 1 compared to total ERK 1 detected in BALB/c CD4+ T-cells.
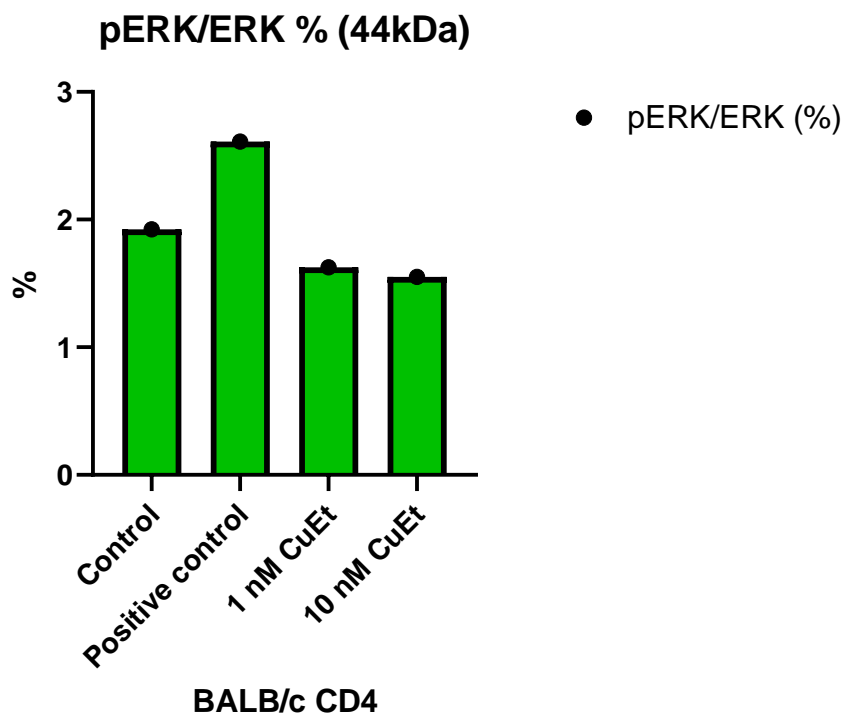
Graph 7 - Percentage quantity of phosphorylated ERK 2 compared to total ERK 2 detected in C57BL6 CD4+ T-cells.
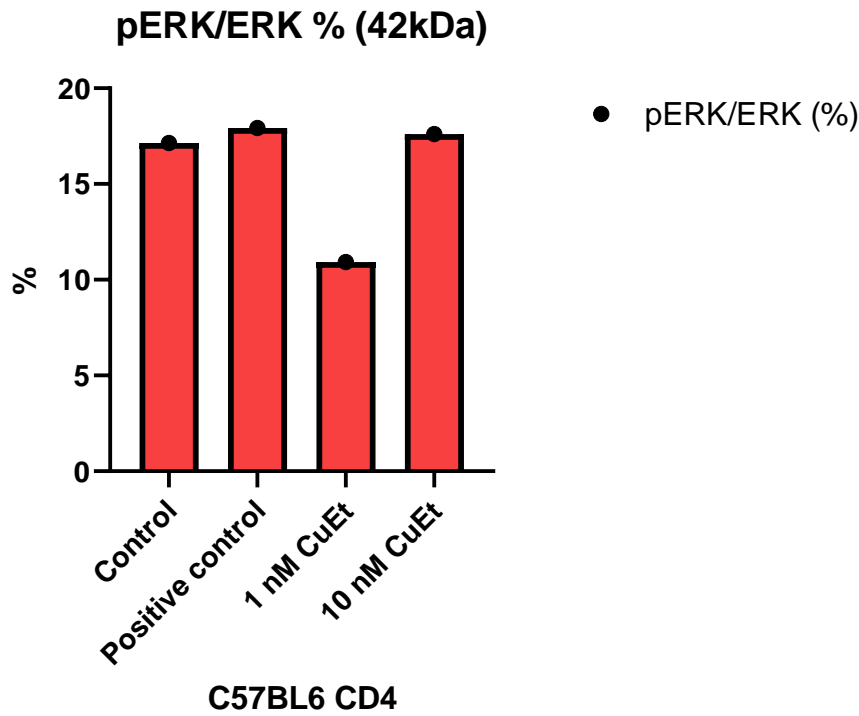

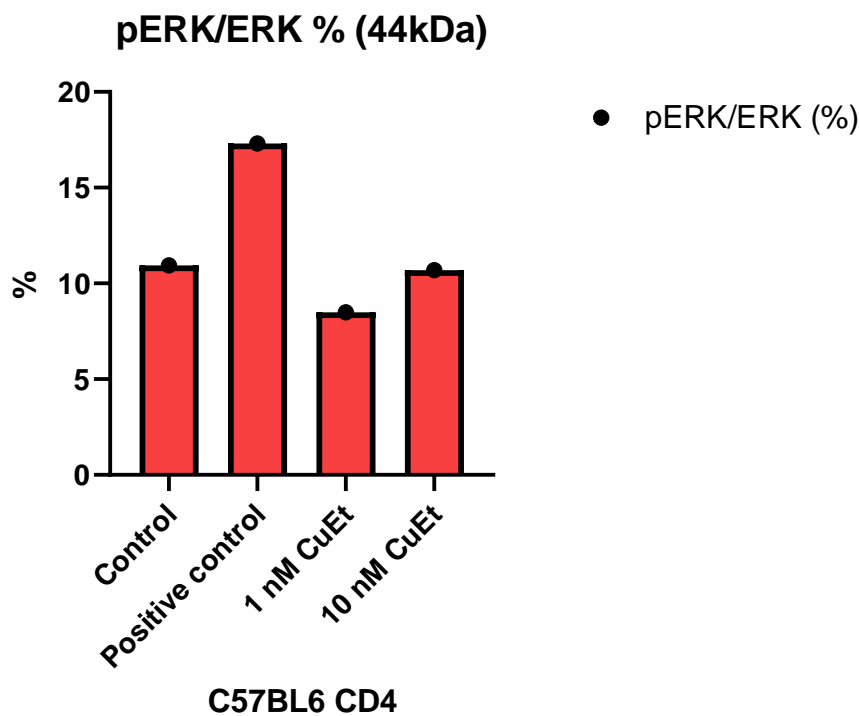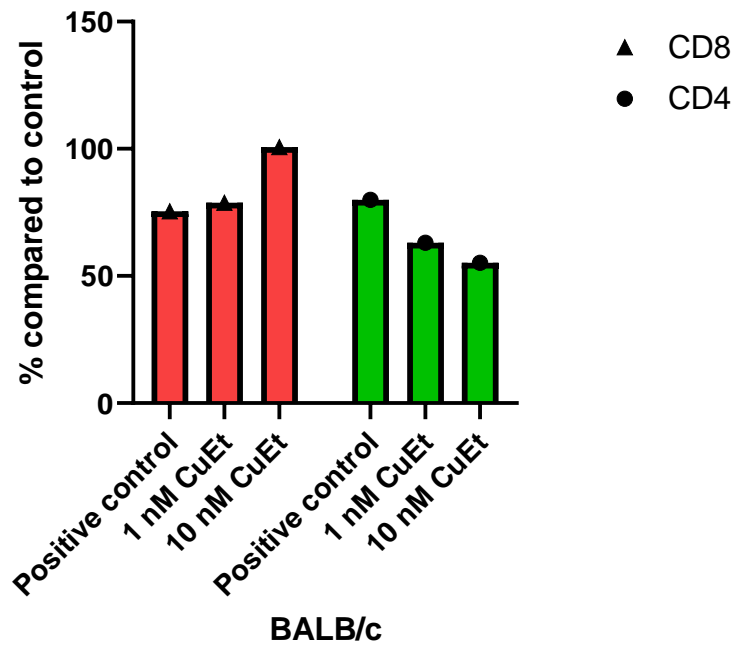*Graph 8 - Percentage quantity of phosphorylated ERK 1 compared to total ERK 1 detected in C57BL6 CD4+ T-cells.*

Graphs 9-12 clearly show that CD8+ cells show higher phosphorylation of ERK1/2 than CD4+ following CuEt treatment. Also, CD4+ cells show an overall lower phosphorylation of ERK

following treatment with CuEt. C57BL6 mice CD8+ cells show higher percentage phosphorylation than negative control following CuEt treatment of both ERK 1 and 2 unlike BALB/c where the percentage increase of phosphorylation compared to negative control only happened in ERK 1 but not in ERK 2.
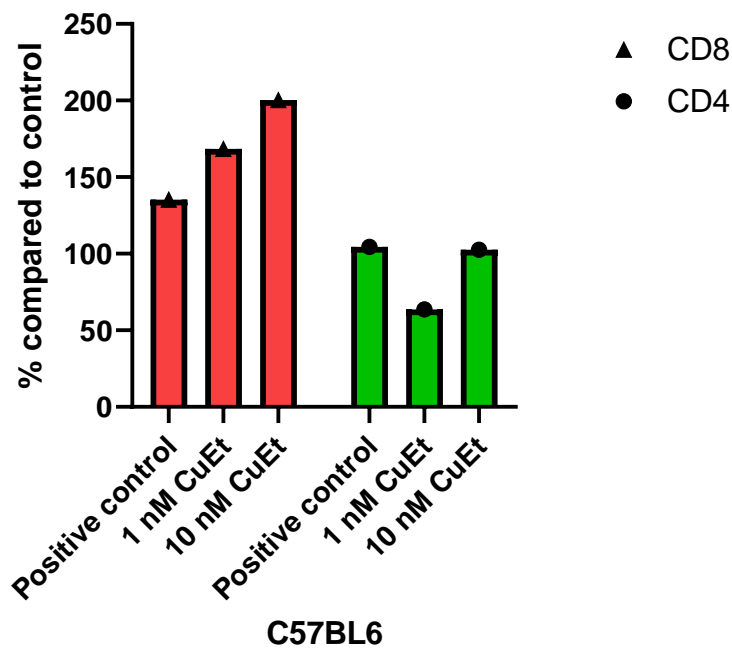

Graph 9 - Percentage of phosphorylated ERK 2 compared to total ERK 2 compared to control in BALB/c.

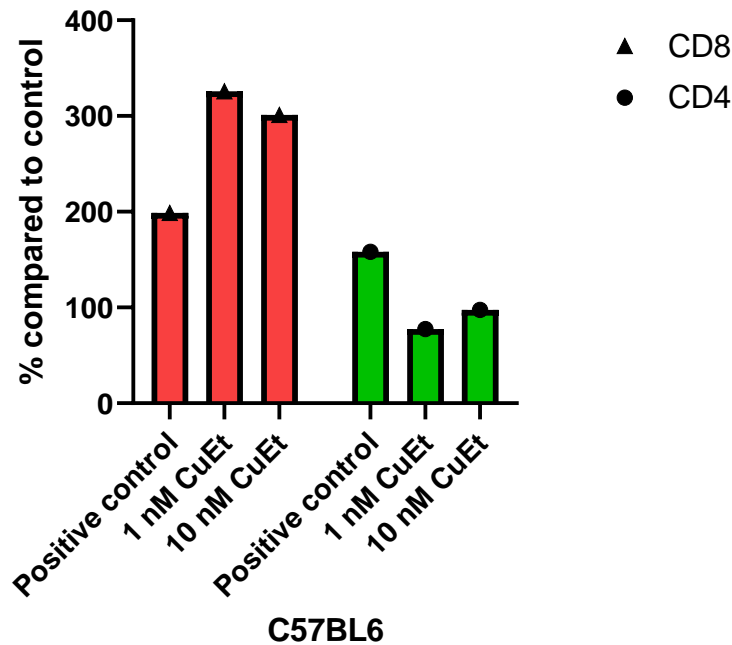# pERK/ERK 44 kDa compared to control
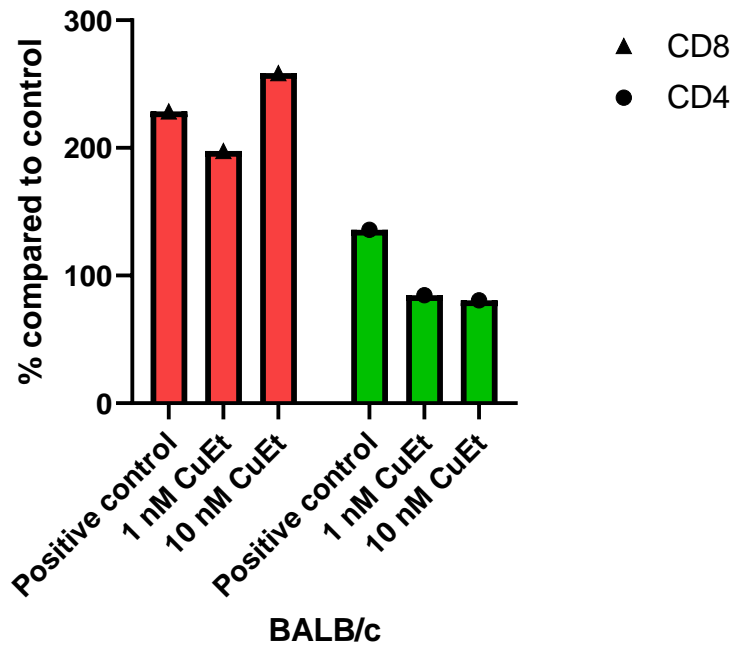
Graph 10 - Percentage of phosphorylated ERK 1 compared to total ERK 1 compared to control in BALB/c.

pERK/ERK 42 kDa compared to control

Graph 11 - Percentage of phosphorylated ERK 2 compared to total ERK 2 compared to control in C57BL6.

pERK/ERK 44 kDa compared to control

Graph 12 - Percentage of phosphorylated ERK 1 compared to total ERK 1 compared to control in C57BL6.

Fig. 12 shows the results of flow cytometry CD314 PE antibody staining. It's clear that there is an increase in CD314 expression following CuEt treatment. Fig. 13 shows the results of flow cytometry anti-perforin PE antibody staining. This effect also shows a clear increase of perforin expression following CuEt treatment. Both CD314 and perforin staining results for both BALB/c and C57BL6 mice strains is compared in graph 13. The MFI (Mean channel fluorescence intensity in logarithmic units) was used to facilitate the analysis of different experiments. There is a significant increase in the expression of both CD314 and perforin after treated with 1 nM CuEt compared to 10 nM CuEt ($P < 0.01$). Both strains reacted to CuEt treatment with an increase in CD314 and perforin expression compared to the control similarly.

Fig. 12 - Extracellular CD314 flow cytometry PE antibody staining BALB/c.. A: Control sample with no treatment. B: Incubated with 1 nM CuEt for 18h. C: Incubated with 10 nM CuEt for 18h.
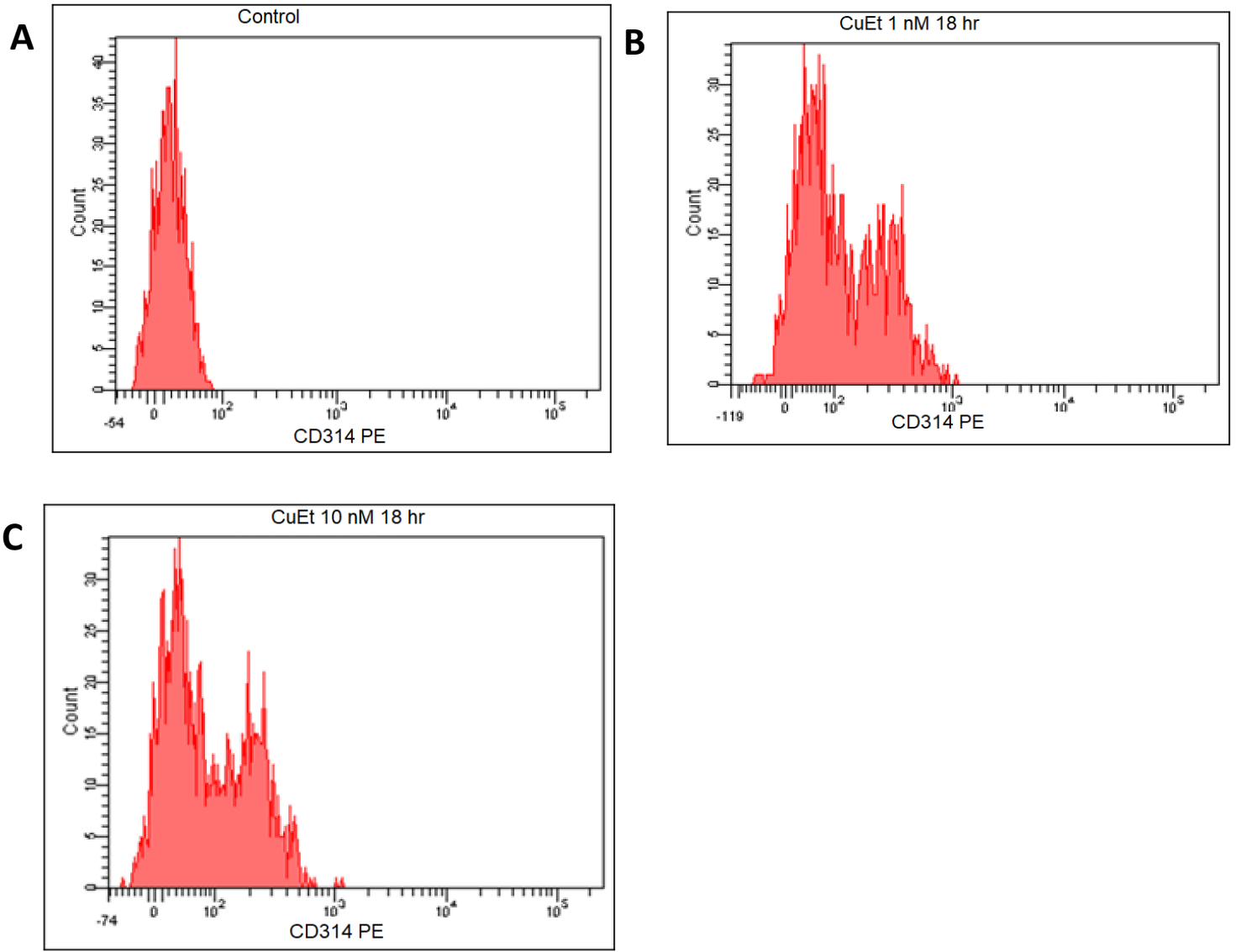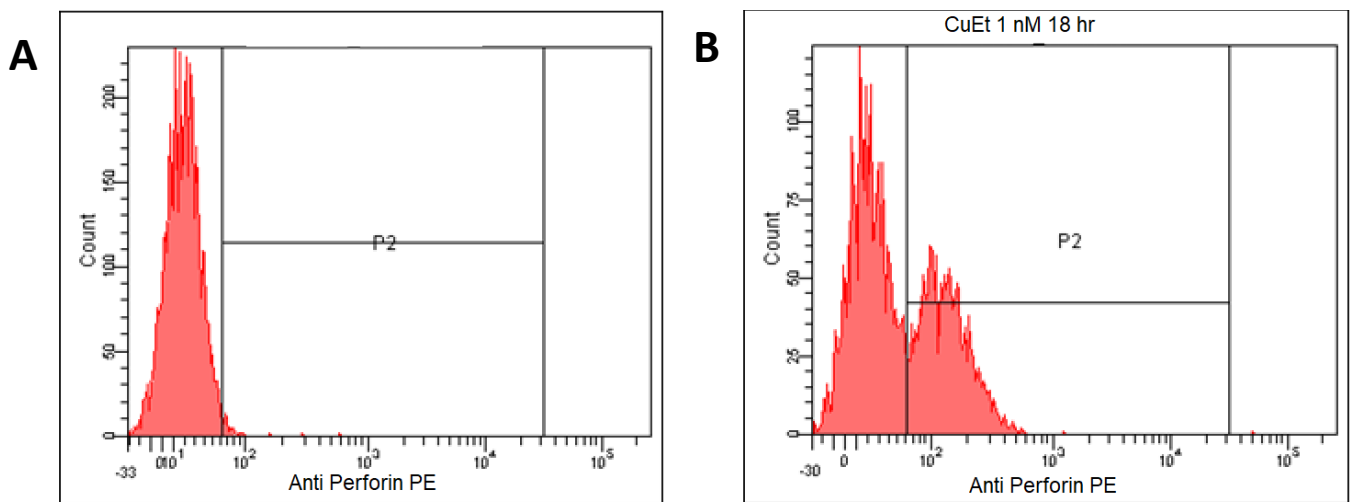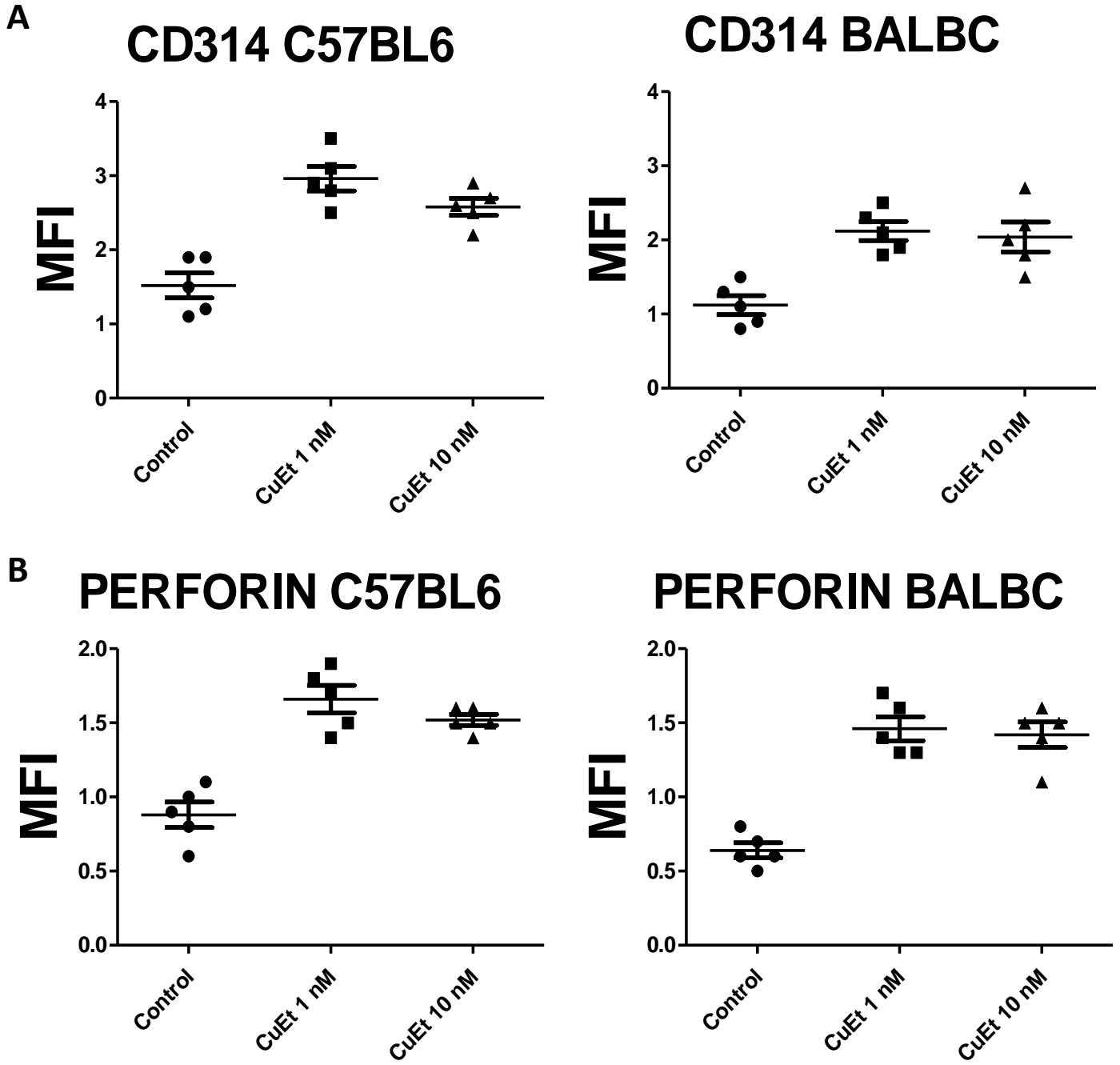

Fig. 13 - Intracellular perforin flow cytometry PE antibody staining C57BL6. A: Control with no treatment B: Incubated with 1 nM CuEt for 18h.

Graph 13 - Mean channel fluorescence intensity in logarythmic units (MFI). A: CD314 in C57BL6 (left) and in BALB/c (right). B: Perforin in C57BL6 (left) and BALB/c (right).

5 Discussion

The results confirmed an ERK1/2 phosphorylation increase in CD8+ cells treated with nanomolar CuEt in both strains. These results support the earlier hypothesis of ERK being activated by CuEt through Lck (fig. 7). This activation was speculated already in 2022 by Bc. Jana Mastná, another student of my supervisor, discovered a higher tyrosine phosphorylation in T-cells upon CuEt activation in her thesis; these results suggested that CuEt primes T cells (J. Mastná, 2022). This finding was the reason ERK was investigated in this thesis. These results were confirmed by the separation of T cells from the splenocytes.

The flow-cytometry results show that perforin and CD314 expression increases in T-cells treated with nanomolar CuEt. The data suggest a significant increase (P<0.01) in the expression when the cells were treated with 1 nM CuEt compared to 10 nM CuEt. This finding is exciting and requires further research. In CD3-stimulated T-cells, the activation and expression of MICA molecules are guided by Lck, Fyn, MEK1/ERK, p38 kinase and calcineurin (L. Molinero *et al.,* 2003). In this case, CuEt activates Lck without going through CD3 activation. This effect has been shown using disulfiram (Q. Wang *et al.,* 2022). These authors showed the lack of effect of disulfiram in Jurkat T cells that lack lck.

Nonetheless, it would have been interesting to see how perforin and CD314 expression would have been affected if an ERK1/2 inhibitor had been used along with CuEt. This effect there are crucial experiments to be done since data not included in this thesis but provided to me by my supervisor from his lab show that the increase in cytotoxicity of T-cells against tumours after treatment with nanomolar concentrations of CuEt is absent in hypoxic conditions. Hypoxic conditions lead to an attenuation of STAT3 and ERK signalisation pathways (R. Teng *et al.,* 2020). This is another piece of information in line with ERK being responsible for the increase of cytotoxicity of T-cells treated with nanomolar concentrations of CuEt.

The relation between ERK1/2 phosphorylation and STAT3 activity also needs to be investigated to confirm the proposed hypothesis (fig.7) of STAT3 activation being enhanced by Lck from 2 different pathways (JAK activation and possibly ERK1/2 out of activation site phosphorylation) (N. Queisser *et al.,* 2017). A study from 2023 by V. Horkova *et al.* reports an important issue; they show two forms of Lck, one bound to the CD8 or CD4 receptor and receptor free. This study also showed that Lck activation can prime a cell to be cytotoxic even before a TCR-mediated activation signal. These results support the possibility of CuEt priming cells without antigens being present. The study also talks about Lck being able to lower the

specificity of antigen recognition needed to provoke a cytotoxic response, possibly increasing the usefulness of non-canonical MHC receptors such as NKG2D, which is increased after CuEt treatment. The results of my thesis experiments suggest that the priming of CD8+ T-cells and the increase of NKG2D and perforin expressed by CuEt treatment is happening in an ERK-dependent manner.

In contrast, CD4+ T-cells didn't show any increase in ERK phosphorylation in either strain, although another signaling pathway could still activate them. The previously mentioned study by V. Horkova *et al.* showed that activation of "free" Lck in the cell is usually enough to influence differentiation and proliferation. CuEt could still influence CD4+ T-cells by activating Lck inside the cells and influencing their differentiation and maturation processes (V. Horkova *et al.,* 2023).

Another crucial experiment that needs to be performed is to measure IL-2 levels as Lck activation often leads to an increased expression which would further enhance cytotoxicity (L. Molinero *et al*., 2003; M. Dosset *et* M. Zanetti, 2022).

The findings of this thesis, and the theses of V. Pokorná and J. Mastná, both from 2022, where they showed induction of NKG2D ligands in tumour cells, show that CuEt increases both NKG2D (CD314) on CD8+ cells and its ligands on tumour cells. This is great for making immune escape harder for tumour cells. The higher expression of perforin confirmed in this thesis along with more NKG2D receptors on T-cells and more ligands on tumour cells, means a better recognition of tumour cells using the NKG2D receptor-ligand interaction as well as more perforin to destroy the targeted cell.

All the experiments performed in this thesis were *in-vitro*. It would also be interesting to inspect the possible change in population and in activation of immune cells of both mice strains if they were inoculated with a tumour and then treated with CuEt.

Finally, is very important to point out that a nanomolar concentration of CuEt in the bloodstream can be realistically achieved *in-vivo*. Therefore, CuEt could become a promising treatment option in the future. More research is needed to shed light on the intricate interaction mechanisms between CuEt in nanomolar concentrations and immune cells.

6 Conclusion

Nanomolar concentrations of CuEt induce perforin and NKG2D (CD314), most probably by the Lck/ERK/NF-κB pathway in CD8+ T-cells. This effect is more robust with 1 nM CuEt than with 10 nM CuEt. ERK isn't activated in CD4+ T-cells by CuEt. Even though the intricate mechanisms and interactions of the immune system and CuEt and cytotoxic response require more research, a mechanism involving NKG2D, and perforin induced by priming the cells with CuEt has been proven. A test for IL-2 secretion and autocrine effect is needed in future research, and a test with ERK inhibitors to confirm the signalling pathway involved.

7 Sources

Anderson, N.M. and Simon, M.C. (2020) 'The tumor microenvironment', Current Biology, 30(16), pp. R921–R925. Available at: https://doi.org/10.1016/j.cub.2020.06.081.

Belo, Y. et al. (2019) 'Unexpected implications of STAT3 acetylation revealed by genetic encoding of acetyl-lysine', Biochimica et Biophysica Acta (BBA) - General Subjects, 1863(9), pp. 1343–1350. Available at: https://doi.org/10.1016/j.bbagen.2019.05.019.

Berkmen, Y.M. and Lande, A. (1975) 'Chest roentgenography as a window to the diagnosis of Takayasu's arteritis', The American Journal of Roentgenology, Radium Therapy, and Nuclear Medicine, 125(4), pp. 842–846. Available at: https://doi.org/10.2214/ajr.125.4.842.

Bizzarri, M. and Cucina, A. (2014) 'Tumor and the Microenvironment: A Chance to Reframe the Paradigm of Carcinogenesis?', BioMed Research International, 2014, pp. 1–9. Available at: https://doi.org/10.1155/2014/934038.

Dosset, M. and Zanetti, M. (2022) 'Disulfiram's journey from rubber vulcanization to T-cell activation', The EMBO Journal, 41(16), p. e111862. Available at: https://doi.org/10.15252/embj.2022111862.

Holdenrieder, S. et al. (2006) 'Soluble MICA in malignant diseases', International Journal of Cancer, 118(3), pp. 684–687. Available at: https://doi.org/10.1002/ijc.21382.

Horkova, V. et al. (2023) 'Unique roles of co-receptor-bound LCK in helper and cytotoxic T cells', Nature Immunology, 24(1), pp. 174–185. Available at: https://doi.org/10.1038/s41590-022-01366-0.

Hsu, A.P. et al. (1993) 'STAT3 Hyper IgE Syndrome', in M.P. Adam et al. (eds) GeneReviews®. Seattle (WA): University of Washington, Seattle. Available at: http://www.ncbi.nlm.nih.gov/books/NBK25507/ (Accessed: 27 July 2023).

Hu, J. et al. (2016) 'Regulation of NKG2D + CD8 + T-cell-mediated antitumor immune surveillance: Identification of a novel CD28 activation-mediated, STAT3 phosphorylation-dependent mechanism', OncoImmunology, 5(12), p. e1252012. Available at: https://doi.org/10.1080/2162402X.2016.1252012.

Huang, C. et al. (2006) 'A Novel NF-κB Binding Site Controls Human Granzyme B Gene Transcription', The Journal of Immunology, 176(7), pp. 4173–4181. Available at: https://doi.org/10.4049/jimmunol.176.7.4173.

Kannappan, V. et al. (2021) 'Recent Advances in Repurposing Disulfiram and Disulfiram Derivatives as Copper-Dependent Anticancer Agents', Frontiers in Molecular Biosciences, 8, p. 741316. Available at: https://doi.org/10.3389/fmolb.2021.741316.

Kim, Y. et al. (2020) 'MICAgen Mice Recapitulate the Highly Restricted but Activation-Inducible Expression of the Paradigmatic Human NKG2D Ligand MICA', Frontiers in Immunology, 11, p. 960. Available at: https://doi.org/10.3389/fimmu.2020.00960.

Levy, D.E. and Darnell, J.E. (2002) 'STATs: transcriptional control and biological impact', Nature Reviews Molecular Cell Biology, 3(9), pp. 651–662. Available at: https://doi.org/10.1038/nrm909.

Levy, D.E. and Lee, C. (2002) 'What does Stat3 do?', Journal of Clinical Investigation, 109(9), pp. 1143–1148. Available at: https://doi.org/10.1172/JCI0215650.

Liu, H. et al. (2020) 'Copper induces hepatic inflammatory responses by activation of MAPKs and NF-κB signalling pathways in the mouse', Ecotoxicology and Environmental Safety, 201, p. 110806. Available at: https://doi.org/10.1016/j.ecoenv.2020.110806.

Lovatt, M. et al. (2006) 'Lck Regulates the Threshold of Activation in Primary T Cells, While both Lck and Fyn Contribute to the Magnitude of the Extracellular Signal-Related Kinase Response', Molecular and Cellular Biology, 26(22), pp. 8655–8665. Available at: https://doi.org/10.1128/MCB.00168-06.

Lu, C. et al. (2021) 'Disulfiram: a novel repurposed drug for cancer therapy', Cancer Chemotherapy and Pharmacology, 87(2), pp. 159–172. Available at: https://doi.org/10.1007/s00280-020-04216-8.

Mastná, Jana. Effect of diethylthiocarbamate copper (CuET) treatment on antigen expression in vitro [online]. Olomouc, 2022 [cit. 2023-07-27]. Dostupné z: https://theses.cz/id/u5u6au/. Bakalářská práce. Univerzita Palackého v Olomouci, Přírodovědecká fakulta. Vedoucí práce prof. Juan Bautista De Sanctis, PhD.

Mitchell, T.J. and John, S. (2005) 'Signal transducer and activator of transcription (STAT) signalling and T-cell lymphomas', Immunology, 114(3), pp. 301–312. Available at: https://doi.org/10.1111/j.1365-2567.2005.02091.x.

Molinero, L.L. et al. (2003) 'Up-regulated expression of MICA on activated T lymphocytes involves Lck and Fyn kinases and signaling through MEK1/ERK, p38 MAP kinase, and

calcineurin', Journal of Leukocyte Biology, 73(6), pp. 815–822. Available at: https://doi.org/10.1189/jlb.0602329.

O'Shea, J.J. et al. (2015) 'The JAK-STAT Pathway: Impact on Human Disease and Therapeutic Intervention', Annual Review of Medicine, 66(1), pp. 311–328. Available at: https://doi.org/10.1146/annurev-med-051113-024537.

O'Shea, J.J., Holland, S.M. and Staudt, L.M. (2013) 'JAKs and STATs in Immunity, Immunodeficiency, and Cancer', New England Journal of Medicine, 368(2), pp. 161–170. Available at: https://doi.org/10.1056/NEJMra1202117.

Osińska, I., Popko, K. and Demkow, U. (2014) 'Perforin: an important player in immune response', Central European Journal of Immunology, 1, pp. 109–115. Available at: https://doi.org/10.5114/ceji.2014.42135.

Pokorná, Vendula. Vliv diethyldithiokarbamátu mědi (CuET) na aktivaci lymfocytů a protinádorovou odpověď [online]. Olomouc, 2022 [cit. 2023-07-27]. Dostupné z: https://theses.cz/id/imghxo/. Bakalářská práce. Univerzita Palackého v Olomouci, Přírodovědecká fakulta. Vedoucí práce prof. Juan Bautista De Sanctis, PhD.

Prajapati, K. et al. (2018) 'Functions of NKG2D in CD8+ T cells: an opportunity for immunotherapy', Cellular & Molecular Immunology, 15(5), pp. 470–479. Available at: https://doi.org/10.1038/cmi.2017.161.

Queisser, N. et al. (2017) 'Aldosterone activates the oncogenic signals ERK1/2 and STAT3 via redox-regulated mechanisms', Molecular Carcinogenesis, 56(8), pp. 1868–1883. Available at: https://doi.org/10.1002/mc.22643.

Ris, M.M., Deitrich, R.A. and Von Wartburg, J.P. (1975) 'Inhibition of aldehyde reductase isoenzymes in human and rat brain', Biochemical Pharmacology, 24(20), pp. 1865–1869. Available at: https://doi.org/10.1016/0006-2952(75)90405-0.

Roskoski, R. (2012) 'ERK1/2 MAP kinases: Structure, function, and regulation', Pharmacological Research, 66(2), pp. 105–143. Available at: https://doi.org/10.1016/j.phrs.2012.04.005.

Skrott, Z. et al. (2017) 'Alcohol-abuse drug disulfiram targets cancer via p97 segregase adaptor NPL4', Nature, 552(7684), pp. 194–199. Available at: https://doi.org/10.1038/nature25016.

Skrott, Z. et al. (2019) 'Disulfiram's anti-cancer activity reflects targeting NPL4, not inhibition of aldehyde dehydrogenase', Oncogene, 38(40), pp. 6711–6722. Available at: https://doi.org/10.1038/s41388-019-0915-2.

Sounni, N.E. and Noel, A. (2013) 'Targeting the Tumor Microenvironment for Cancer Therapy', Clinical Chemistry, 59(1), pp. 85–93. Available at: https://doi.org/10.1373/clinchem.2012.185363.

Taniguchi, K. and Karin, M. (2018) 'NF-κB, inflammation, immunity and cancer: coming of age', Nature Reviews Immunology, 18(5), pp. 309–324. Available at: https://doi.org/10.1038/nri.2017.142.

Teng, R. et al. (2020) 'Hypoxia Impairs NK Cell Cytotoxicity through SHP-1-Mediated Attenuation of STAT3 and ERK Signaling Pathways', Journal of Immunology Research, 2020, pp. 1–14. Available at: https://doi.org/10.1155/2020/4598476.

Tian, Z.J. and An, W. (2004) 'ERK1/2 contributes negative regulation to STAT3 activity in HSS-transfected HepG2 cells', Cell Research, 14(2), pp. 141–147. Available at: https://doi.org/10.1038/sj.cr.7290213.

Valentini, Viktor. Effect of disulfiram metabolites on NK and T cell cytotoxic activity against tumor resistant cell lines [online]. Olomouc, 2021 [cit. 2023-07-27]. Dostupné z: https://theses.cz/id/d9ymuf/. Bakalářská práce. Univerzita Palackého v Olomouci, Přírodovědecká fakulta. Vedoucí práce prof. Juan Bautista De Sanctis, PhD.

Wang, Q. et al. (2022) 'Disulfiram bolsters T-cell anti-tumor immunity through direct activation of LCK-mediated TCR signaling', The EMBO Journal, 41(16), p. e110636. Available at: https://doi.org/10.15252/embj.2022110636.

Xue, C. et al. (2023) 'Evolving cognition of the JAK-STAT signaling pathway: autoimmune disorders and cancer', Signal Transduction and Targeted Therapy, 8(1), p. 204. Available at: https://doi.org/10.1038/s41392-023-01468-7.

Yourick, J.J. and Faiman, M.D. (1991) 'Disulfiram metabolism as a requirement for the inhibition of rat liver mitochondrial low Km aldehyde dehydrogenase', Biochemical Pharmacology, 42(7), pp. 1361–1366. Available at: https://doi.org/10.1016/0006-2952(91)90446-C.

Zhou, J. et al. (2002) 'A Role for NF-κB Activation in Perforin Expression of NK Cells Upon IL-2 Receptor Signaling', The Journal of Immunology, 169(3), pp. 1319–1325. Available at: https://doi.org/10.4049/jimmunol.169.3.1319.

Zloza, A. et al. (2012) 'NKG2D signaling on CD8+ T cells represses T-bet and rescues CD4-unhelped CD8+ T cell memory recall but not effector responses', Nature Medicine, 18(3), pp. 422–428. Available at: https://doi.org/10.1038/nm.2683.